DEVELOPMENT OF UNIVERSAL STOICHIOMETRIC COEFFICIENTS FOR MODELING MICROALGAL CULTIVATION SYSTEMS

BY

STEPHANIE MARIE SCHRAMM

THESIS

Submitted in partial fulfillment of the requirements
for the degree of Master of Science in Environmental Engineering in Civil Engineering
in the Graduate College of the
University of Illinois at Urbana-Champaign, 2018

Urbana, Illinois

Adviser:

Assistant Professor Jeremy Guest

ABSTRACT

Biological treatment processes at water resource recovery facilities (WRRFs; a.k.a. wastewater treatment plants) are approaching the limit of technology for nitrogen and phosphorus removal. Algae treatment technologies have the ability to remove additional nitrogen and phosphorus, thereby lowering the effluent nutrient discharge level at WRRFs. A critical challenge for the adoption of algal technologies, however, is the lack of robust algae modeling platforms for wastewater treatment that can predict process performance under fluctuating reactor conditions and despite the inevitable biodiversity of influent wastewater. One necessary step towards improved modeling capabilities for algae treatment systems is the development of generalizable model parameters, such as stoichiometric parameters – like those used in the International Water Association's (IWA's) Activated Sludge Models (ASMs). This work introduces universal stoichiometric coefficients for algal process modeling derived from the conserved enzymatic properties for seven algae species using 11 genome-scale models. The model parameters include yield coefficients for algae grown under various energy inputs (photoautotrophic and heterotrophic), nitrogen sources (ammonia and nitrate), and carbon sources (inorganic, acetate, and glucose) as well as stoichiometric parameters for the accumulation of storage compounds (starch and lipids). Generalizable stoichiometric parameters based on conserved metabolic properties would bolster accuracy and the accessibility of algal process models. This will help promote the use of algal technologies by wastewater design engineers and utilities to improve the effluent quality at water resource recovery facilities.

ACKNOWLEDGEMENTS

TABLE OF CONTENTS

CHAPTER 1. Introduction

Nutrient levels in water bodies play a critical role in the health of aquatic ecosystems. High nitrogen and phosphorus levels in natural waters can lead to eutrophication, or an increase growth in algae and cyanobacteria. The increase in phototrophic organisms and their subsequent degradation causes there to be limited oxygen available as well as cyanotoxins in the water, which in turn kills higher level organisms such as fish (Chislock, 2013). There have been several eutrophication problems worldwide that have had significant impact on the economy and human well-being. Hypoxic zones in the Gulf of Mexico, Chesapeake Bay, and Lake Taihu have created dead zones where fish can no longer live (Duan et al., 2009; Rabalais, Turner, & Wiseman, 2002; Ruhl & Rybicki, 2010); the decline in fish availability causes several issues for the seafood industry and fisheries such as an increase in forced migration and predation among species (Rabalais et al., 2002). Eutrophication can also cause an increase in toxins produced in the water by algae and cyanobacteria species. With an increase in toxin levels, water bodies have limited recreational use and can pose a health risk to communities. For example, Lake Erie commonly has do-not-swim zones due to increased toxins during the summer months (Rinta-Kanto et al., 2009). In addition, harmful algae blooms prior to the Beijing Olympics caused military personnel and volunteers to have to come clean up the Olympic sailing venue (Conley et al., 2009). Furthermore, several outbreaks of Pyrodinium blooms have caused illness to spread throughout the Philippines due to the high consumption of shellfish that have eaten toxic algae (Hallegraeff, 1993).

One of the largest discharging units to natural water bodies are water resource recovery facilities, also known as wastewater treatment plants (Ruhl & Rybicki, 2010). Water resource recovery facilities take incoming wastewater from homes, industrial plants, office buildings, and other locations and remove organic carbon as well as nitrogen and phosphorus before discharging the water to a natural water body. The quality of effluent water being discharged by the WRRF can have a significant impact on the aquatic ecosystem in the receiving water body by possibly enhancing eutrophication or introducing unnatural chemical species into the water. WRRFs need to operate with the goal of limiting eutrophication and harmful algal blooms in natural systems (Paerl et al., 2011). The Environmental Protection Agency (EPA) controls the level of organic carbon, nitrogen, and phosphorus that can be found in WRRF effluent so that natural water bodies are exposed to minimal harm in the United States. Throughout the years, the EPA is continuing to lower the effluent discharge limits for nitrogen and phosphorus concentration so that society

can have cleaner water in our communities (Carey & Migliaccio, 2009). Nitrogen is typically removed at WRRFs through the process of nitrification and denitrification. Together these processes convert inorganic nitrogen in the water into dinitrogen gas; the limit of technology for nitrification and denitrification allows effluent levels to reach approximately 3 mg N L^{-1} (Bott and Parker, 2011; U.S. EPA, 2015). At most WRRFs, phosphorus is commonly removed through chemical processes or enhanced biological phosphorus removal (EBPR), both of which can achieve effluent quality of 0.1 mg P L^{-1} (Tchobanoglous, Burton, Stensel, & Metcalf & Eddy, 2003; U.S. EPA, 2015).

As effluent nitrogen and phosphorus limits become more stringent, wastewater utilities are looking for new technologies to help achieve lower nitrogen and phosphorus effluent concentrations. Algal technologies have advantageous properties for use in WRRFs. Algae wastewater treatment technologies have the possibility to lower effluent nutrient concentrations by removing inorganic and organic nutrients (nitrogen and phosphorus) that are not easily removed with current WWRF systems. Algal technologies have the potential to also produce valuable coproducts such as animal feed, fertilizers, and bioenergy feed-stocks.

A significant hurdle to the widespread application of algal technologies at WRRFs is the replication of algae cultivation processes (Guest, van Loosdrecht, Skerlos, & Love, 2013) Water resource recovery facilities are found in various geographical locations and have varying influent streams. Wastewater is beneficial to use as a medium for algae cultivation because of its high nutrient level and the economic feasibility of linking the two processes. However, due to variability in composition and the inevitable biodiversity of wastewater, achieving an axenic culture within the system is not feasible. Because of possible differences in mixed microalgae communities at any given WRRF, it is beneficial to have process design parameters that are conserved across algae species, allowing for the replication of algal technologies regardless of WRRF influent and location. To increase the utilization of algal biological nutrient removal technologies in industry, it is necessary to understand the metabolic properties under various energy inputs (photoautotrophic and heterotrophic), carbon sources (carbon dioxide, acetate, and glucose), nitrogen sources (ammonia and nitrate), and the conserved qualities of these metabolic properties among various algae species. A universal approach needs to be taken to understand how algae of various species uptake nutrients and store energy from wastewater so that more accurate and reproducible models can be developed for algae technologies used in wastewater treatment.

The objective of this thesis is to show the development of universal stoichiometric properties for algae process modeling in the context of wastewater treatment. The background section will give a broad view of modeling in the wastewater treatment industry. How algae modeling fits into wastewater modeling platforms will be addressed, including current processes, gaps in the research field, and promising future directions. Chapter 3, Enzyme Conservation, will explore how species-specific algae metabolic data can be adapted for mixed algal community process modeling by showing the steps taken to elicit data demonstrating the conservation of metabolic processes among algae species. With the enzyme conservation basis shown in chapter 3, chapter 4 will dive into the process of lumped pathway metabolic modeling or taking enzyme conservation data and developing yield coefficients for key metabolic processes in algal treatment technologies. Conclusions that can be drawn from the work as well as the engineering significance of the research will be explained in chapters 5.

CHAPTER 2. Background

2.1 Current Wastewater Treatment Modeling Practices. The wastewater treatment industry has models developed for processes common to most WRRFs, including nitrogen and phosphorus removal, known as the activated sludge models (ASMs). The activated sludge models have driven wastewater treatment modeling research in a positive and productive direction since their development. The ASM modeling format has allowed the wastewater modeling community to come together and follow common nomenclature and a comprehensive layout of the model known as the Petersen matrix (Henze, Gujer, Mino, & van Loosdrecht, 2000; Petersen 1965). The consistency among the wastewater industry has driven the field forward and also allowed for cohesiveness between all stakeholders from operators to consultants. The activated sludge models include kinetic rate equations and stoichiometric coefficients along with typical values used in the models for kinetic constants and stoichiometric coefficients (Henze et al., 2000). The ASMs give empirical yield coefficient values as a preliminary estimate for running the model, stating that experiments should be completed to develop parameters, such as stoichiometric yield coefficients, for specific WRRFs (Henze et al., 2000). Differences in modeling parameters among WRRFs are believed to be due to environmental influences such as changes in pH, temperature, and inhibitory and/or stimulatory compounds in the influent (Henze, 1986). Considering the future of the wastewater treatment modeling industry, a push for more mechanisms based on biochemical properties instead of empirical values is important (Daigger, 2011).

2.2 Algae Treatment Technologies in Wastewater Modeling. The wastewater industry has exceled in developing a universal modeling structure for biological nutrient removal processes, including nitrification, denitrification, and enhanced biological phosphorus removal. The modeling of algae systems for wastewater treatment has not been as directed in creating a format similar to the ASMs to follow for the algae modeling research community. In order for algae technologies to take off, the modeling of microalgal systems needs to become increasingly universal like the ASMs. Currently, most processing parameters in industry for algae technologies are based on experimental data and presented in various formats (Baroukh, Muñoz-Tamayo, Steyer, & Bernard, 2015; Wágner et al., 2016). Experimental data is necessary for validating models and understanding algae metabolism, however, processing parameters from experimental studies can be difficult to utilize universally. While these values are extremely useful for pure culture and single species applications, they are not as useful for wastewater treatment which cannot use pure culture or single species cultivation due to the biodiversity of wastewater. It is difficult to utilize

empirical data in a mixed culture system because experimental studies would have to be completed for each new community formed, requiring intensive resources and time most WRRFs do not have. Generalizable model properties are needed to advance the use of algae treatment systems.

2.3 Metabolic Modeling of Algal Systems. One way to develop generalizable model properties is to develop model properties based on the species' metabolism instead of empirical, experimental data. Metabolic modeling considers the processes being completed inside the microorganism (i.e. Glycolysis, fatty acid synthesis, oxidative phosphorylation, etc.) instead of looking at the microorganism as a "black box" with only inputs and outputs and no insight into what goes on inside the cell (C. Yang, Hua, & Shimizu, 2000). Similar to current wastewater treatment process models, kinetic and stoichiometric properties are the two key properties needed for modeling growth in algal cultivation systems. Kinetic properties vary with time, making it difficult to incorporate kinetic properties into metabolic models. Stoichiometric properties are modeled in steady state, which allows for the analysis of yield while considering the whole metabolic network (Shastri & Morgan, 2005). Developing stoichiometric coefficients, specifically yield coefficients based on the metabolism of microalgae, is a step needed for creating generalizable algae process models. Metabolic modeling uses biochemical data representing a species' or communities' metabolism to develop stoichiometric parameters for processing operations. Metabolic models range from whole genome scale models (Chang et al., 2011) to specific storage process models (Filipe & Daigger, 1999). Although there is a push and consensus that metabolic information needs to be incorporated into algae process models (Boyle & Morgan, 2009), very few models have actually taken metabolism into account during model development (Baroukh, Muñoz-Tamayo, Steyer, & Bernard, 2014; Fleck-Schneider, Lehr, & Posten, 2007; Guest et al., 2013). Metabolic modeling has the potential to limit the number of model inputs and provide parameters that are viable across various components of microalgae growth important to the wastewater treatment industry. The energy input for growth (photoautotrophic, heterotrophic, and mixotrophic) (C. Yang et al., 2000; Zuñiga et al., 2018) can be represented by metabolic models along with differences in nitrogen source (Perez-Garcia, Bashan, & Esther Puente, 2011), nitrogen availability (Hu et al., 2008; Yanqun Li, Horsman, Wang, Wu, & Lan, 2008), and the accumulation of storage compounds (Baroukh et al., 2014; Guest et al., 2013).

2.4 Growth Conditions. Microalgae have the capability to grow under photoautotrophic, heterotrophic, and mixotrophic conditions. Photoautotrophy is the most common growth modeled. During photoautotrophic growth, microalgae harness energy from sunlight and take up carbon

dioxide, converting inorganic carbon to organic carbon that makes up the microalgae biomass. Photoautotrophic growth is most similar to plant growth. Heterotrophic growth is when cells use an external organic carbon source for both energy and growth. In this study, heterotrophic growth on acetate and glucose was considered. Heterotrophic growth of algae has been found to have higher productivities at lower operational costs (Liang, Sarkany, & Cui, 2009; Xiong, Liu, Wu, Yang, & Wu, 2010). Heterotrophic models are becoming more populous in recent years, but there is still a lot of work to be done to understand the kinetic and stoichiometric properties of heterotrophic algae growth. Mixotrophic growth occurs when both photoautotrophic and heterotrophic growth conditions are taking place. Mixotrophic growth models are usually formed by summing values from both photoautotrophic and heterotrophic models (Adesanya, Davey, Scott, & Smith, 2014; Boyle & Morgan, 2009; Lee, Jalalizadeh, & Zhang, 2015) Like heterotrophic growth, there are also few models available considering mixotrophic growth, however mixotrophic growth has the potential to have higher algae biomass yield than heterotrophic conditions with a lower cost than photoautotrophic growth. Due to the higher yield and lower cost associated with mixotrophic growth, there is a growing interest in modeling mixotrophic algal cultivation (Boyle & Morgan, 2009).

2.5 Nitrogen. For the present study, three different nitrogen nutrient conditions were considered: nitrogen in the form of ammonia (nitrogen replete), nitrogen in the form of nitrate (nitrogen replete), and no nitrogen present (nitrogen deplete). In wastewater, the two most common forms of nitrogen that are focused on for removal are ammonia and nitrate (Tchobanoglous et al., 2003). Nitrate and ammonia are the also two target nitrogen species for removal in wastewater treatment due to the harm nitrate and ammonia can cause in natural water bodies if left in the effluent of WRRFs.

Besides considering the most common forms of nitrogen present in wastewater treatment plants, the condition of nitrogen deplete, or no nitrogen in the system, was also considered. Nitrogen depletion is important to consider because when nitrogen is not present in the system, it promotes the accumulation of algal storage products, such as carbohydrates and lipids (Hu et al., 2008; Perez-Garcia et al., 2011). Carbohydrates and lipids produced by microalgae are considered promising feedstocks for biofuels (Balaji, Gopi, & Muthuvelan, 2013; Chisti, 2008) and bio-based products such as bioplastics (Balaji et al., 2013).

When looking at modeling nitrogen in algae systems, there are some factors to consider. For instance, the uptake of nitrate and ammonia by the algae cell requires different amounts of energy.

Ammonia can be taken up and directly used in its given form for protein and biomass synthesis within the cell. Nitrate, however, must be converted to a usable form once it enters the cell. This conversion causes the cell to put more energy towards nitrogen accumulation when nitrate is the nitrogen source present, making less energy available to the cell for other purposes such as growth (Geider & Osborne, 1989; Eppley, 1969). When modeling algae process systems, the difference in energy requirement between nitrogen sources is an important consideration to understand cell growth and energy consumption.

2.6 Storage Polymers. The two storage polymers focused on for this study are carbohydrates and lipids. Carbohydrates have several qualities that lead to microalgae technologies being promising for the wastewater treatment industry. For example, carbohydrates can become a potential biofuel source. Carbohydrates can be converted to bioenergy via multiple processes. Anaerobic digestion converts carbohydrates from algae into methane and carbon dioxide gas; the methane can be harnessed and used for power generation. Anaerobic fermentation is another common carbohydrate processing technique in which the carbohydrates produced in algae are broken down into sugars and fermented into bioethanol (Markou, Angelidaki, & Georgakakis, 2012).

Besides carbohydrates being a biofuel feedstock, carbohydrates are also important for algae nitrogen uptake during diurnal cycles. The accumulation of carbohydrates within the cell help algae cells outcompete other non-photoautotrophic species in the absence of light by allowing the cell to continue to grow and take up nutrients in the absence of light by metabolizing carbohydrates (van Aalst-van Leeuwen, Pot, van Loosdrecht, & Heijnen, 1997a). Lipid storage molecules can also be used for this purpose; however, it is harder to mobilize and metabolize lipids within the cell; lipid storage molecules are less dynamic than carbohydrate storage molecules (Guest et al., 2013).

Lipids are seen as another important storage polymer to model in algae species. Lipids can be converted into biodiesel via several processes; the most commonly considered method for lipid separation from biomass is hydrothermal liquefaction (HTL). HTL works by thermochemically converting whole wet algal cells into biodiesel (Leow, R. Witter, et al., 2015; Yalin Li et al., 2017). A lipid solvent extraction is another biodiesel production method that can be completed on dried algal biomass to extract lipids (Mata, Martins, & Caetano, 2010). After the lipids are extracted, transesterification is one process used to convert the algae lipids into biodiesel by a multistep reaction that converts triglycerides (algae lipids) to glycerol (Mata et al., 2010).

Storage polymers are very important components of algal biomass and metabolism, however, there has not been a lot of research done around the kinetic and stoichiometric properties of carbohydrates and lipids in algae. A recent (2014) study found only nine algae process models that had any focus on carbon storage (Baroukh et al., 2014). In addition, only two of these nine models modeled carbon storage in microalgae using metabolic properties (Fleck-Schneider et al., 2007; Guest et al., 2013). More work needs to focus on the modeling properties of carbon storage compounds; storage compounds are important to algae growth, nutrient uptake, and the processing of algae into valuable products such as algae-based biofuels.

2.7 Metabolic Data Types. With the advances in genomic analyses and the increased number of molecular tools available allowing for full genomic annotations of algae species (Koskimaki, Blazier, Clarens, & Papin, 2013; Tirichine & Bowler, 2011), it is now possible to gain a better understanding of the algal metabolism. Full scale genomic annotations of algae species have been primarily used for understanding the effects of genetic modifications to algae species for increased lipid and/or carbohydrate production (Carrier et al., 2018; Vieler et al., 2012). While genetic manipulation is useful in some aspects of the industry, full scale genomic data has found to be too complex, hard to manipulate, and species specific for wastewater treatment process modeling. In the context of wastewater treatment with mixed algae communities, genomic analyses cannot easily be used as a form of metabolic data. Metabolic Reconstructions of full genome annotations are one step taken to provide more refined data for algal metabolisms (Boyle & Morgan, 2009; Gomes de Oliveira Dal'Molin, Quek, Palfreyman, & Nielsen, 2011; Imam, Schäuble, Valenzuela, de Lomana, et al., 2015). A metabolic reconstruction for a given organism uses available experimental knowledge about the metabolism of a given species along with genome annotation for the species to determine metabolic pathways present in a given species and the reactions making up those pathways that are performed by certain enzymes (Chang et al., 2011). Metabolic reconstructions give an overall view of the species metabolism, however they are very complex, commonly containing about 1000-2000 metabolites and anywhere from 300 to 2000 reactions (Gomes de Oliveira Dal'Molin et al., 2011; Imam, Schäuble, Valenzuela, de Lomana, et al., 2015; Wu, Xiong, Dai, & Wu, 2015; Zuñiga et al., 2018). Metabolic reconstructions have been used for metabolic engineering manipulations, such as increasing the flux through a preferred pathway and analyzing species through flux balance analysis (Baroukh et al., 2015; Boyle & Morgan, 2009; Guarnieri et al., 2011; Shastri & Morgan, 2005). Metabolic reconstructions are useful in these instances for pure culture applications, but do not work well for mixed community analyses and modeling, which is the type of modeling needed in wastewater

treatment. Even though the model created by the metabolic reconstruction is difficult to use for multiple species as is, it is useful for determining the conservation of given enzymes across algae species.

CHAPTER 3. Enzyme Conservation

3.1 Algae Species Considered. Eleven microalgae metabolic reconstruction data sets were found to be published with attached enzyme data and were analyzed for seven different algae species. The algae species include: *Chlamydomonas reinhardtii* (Boyle & Morgan, 2009; Chang et al., 2011; Gomes de Oliveira Dal'Molin et al., 2011; Imam, Schäuble, Valenzuela, de Lomana, et al., 2015; Manichaikul et al., 2009), *Nannochloropsis oceanica* (Vieler et al., 2012), *Chlorella protothecoides* (Wu et al., 2015)*, Chlorella vulgaris* (Zuñiga et al., 2018)*, Chlorella variabillis* (Juneja, Chaplen, & Murthy, 2016), *Ostreococcus lucimarinus*, and *Ostreococcus tauri* (Krumholz, Yang, Weisenhorn, Henry, & Libourel, 2012). The universal enzymatic properties of algae were considered across the seven species for sixteen relevant metabolic pathways.

3.2 Metabolic Pathways Considered. Sixteen pathways were chosen to make up the metabolic model of algae metabolism **(table 3.1).** The 16 pathways were chosen by looking at metabolic reconstruction models and understanding what metabolites would be important for achieving the desired outcome including nutrient assimilation from wastewater and energy compound storage. Even though models created by metabolic reconstructions are complex and hard to manipulate, the information is useful for developing yield coefficients for use in engineering operation and design based on the metabolic properties of algae. The major algae metabolic pathways included are involved in: central carbon metabolism, nitrogen assimilation, phosphorus assimilation, lipid synthesis and storage and carbohydrate synthesis and storage and can be found in **table 3.1.**

Table 3.1 Included Metabolic Pathways

1	Glycolysis	9	Glyoxylate cycle
2	Pentose phosphate pathway	10	Beta oxidation
3	Tricarboxylic acid (TCA) cycle	11	Fatty acid synthesis
4	Photosynthesis	12	Carbohydrate (starch) synthesis
5	Calvin cycle	13	Carbohydrate (starch) degradation
6	Photorespiration	14	Triacylglycerol (lipid) synthesis
7	Ammonia assimilation	15	Triacylglycerol (lipid) degradation
8	Nitrate assimilation	16	Gluconeogenesis

Three conditions were analyzed by conducting a literature review of algae metabolic reconstructions: photoautotrophic growth, heterotrophic growth, and nitrogen limited conditions. During photoautotrophic growth, sunlight provides energy to the cell and carbon dioxide is the carbon source for the algae cell. During heterotrophic growth, no light is present and both the energy and carbon source for the algae is organic carbon, such as glucose or acetate. When little

to no nitrogen is present in the algae media, the algae cell is said to be under nitrogen limited conditions.

Several metabolic reconstructions that were analyzed have been formed *in silico* under the three conditions described above. The metabolic reconstructions were commonly broken down into metabolic pathways during previous analyses in order to see which pathways were expressed and not expressed under specific growth conditions. While some metabolic pathways showed clear trends of expression that varied under the different growth conditions, other pathways did not show any trends at all. Brief descriptions of the overall trends of expression in metabolic pathways are provided below.

Glycolysis, or the Embden–Meyerhof–Parnas (EMP) pathway, has flux under all three conditions. Light intensity and availability to algae has little effect on glycolysis, making the flux close to constant under photoautotrophic, heterotrophic and nitrogen limited conditions (Imam, Schäuble, Valenzuela, de Lomana, et al., 2015; C. Yang et al., 2000). However, different molecules may enter and leave the glycolysis pathway under the three conditions. For example, under photoautotrophic conditions, glyceraldehyde-3-phosphate produced from photosynthesis enters glycolysis and under heterotrophic conditions with glucose as the organic carbon source, glucose will be converted into glucose-6-phosphate which will then go through glycolysis.

The pentose phosphate pathway has more variation in flux and activity under the various conditions. The pentose phosphate pathway is most active under heterotrophic conditions, or when no light is available to the cell (Boyle & Morgan, 2009; Perez-Garcia et al., 2011; Wu et al., 2015; Xiong et al., 2010) In addition, the pentose phosphate pathway has increased activity under nitrogen limitation (Imam, Schäuble, Valenzuela, López García de Lomana, et al., 2015).

Both light intensity and nitrogen availability do not have significant effects on the tricarboxylic acid (TCA) cycle (Perez-Garcia et al., 2011; Xiong et al., 2010; C. Yang et al., 2000). The TCA cycle is similar to glycolysis in that it has flux under all three conditions: photoautotrophic, heterotrophic, and nitrogen limited. Also, like glycolysis, different molecules can enter the TCA cycle at different points of the cycle depending on the condition the cell is exposed to.

Photosynthesis is active under photoautotrophic conditions and not active under heterotrophic conditions because photosynthesis always needs a light source for energy (Wu et al., 2015; C.

Yang et al., 2000). When nitrogen is the flux of photosynthesis decreases; but the metabolic pathway is still active (Radakovits et al., 2012; Xiong et al., 2010). Photosynthesis can also have an increased or decreased flux based on the type of light the algae is exposed to such as white light, red light, blue light, or a combination of light types (Juneja et al., 2016).

After photosynthesis, the carbon compounds produced enter the Calvin-Benson cycle. The Calvin-Benson cycle increases in flux when light is present, or during photoautotrophic conditions (Boyle & Morgan, 2009; Shastri & Morgan, 2005; Wu et al., 2015; C. Yang et al., 2000). The cycle decreases in flux when light is not present, but it is still active (Perez-Garcia et al., 2011; C. Yang et al., 2000).

Photorespiration occurs when oxygen is utilized by the first enzyme of the Calvin-Benson cycle (ribulose- 1,5-biphosphate carboxylase/oxygenase) instead of carbon dioxide. Photorespiration commonly occurs when the oxygen saturation in the media is above 7.19 gO_2 m^{-3} (Chisti, 2008; Solimeno et al., 2015) There is a lot of conflicting modeling assumptions around including or excluding photorespiration in a model; more research needs to be done in order to truly understand the significance of the photorespiratory pathway and when it is active and not active in regards to light and nitrogen availability (Arnold & Nikoloski, 2013; Baroukh et al., 2015). Photorespiration was analyzed for enzyme conservation but is not included as a pathway in the model developed from metabolic reconstruction data due to the fact that wastewater treatment algae technologies being considered will have oxygen levels below saturation (C. Yang et al., 2000).

Nitrogen assimilation into the cell is important both for nutrient removal in WRRFs and for cell growth. Two forms of nitrogen that can be assimilated by algae cells were analyzed: nitrate and ammonia. Both nitrate assimilation and ammonia assimilation in the algae cell increase in flux when light is present to the system (Imam, Schäuble, Valenzuela, López García de Lomana, et al., 2015). Nitrate and ammonia assimilation are also both dependent on the type of nitrogen available to the cell. For example, if ammonia is present to the cell, the flux of nitrate assimilated into the algal metabolism will decrease because ammonia is the preferred nitrogen source for algae (Perez-Garcia et al., 2011). Similar to photosynthesis, the type of light available to the system may also play a role in the flux of nitrate and ammonia assimilation (Kamiya & Kowallik, 1987).

The glyoxylate cycle allows the cell to metabolize acetate. The flux through the glyoxylate cycle increases under heterotrophic conditions when acetate is the organic carbon source (Boyle & Morgan, 2009; Perez-Garcia et al., 2011; Shastri & Morgan, 2005). When nitrogen is limited in the system, the activity of the glyoxylate cycle decreases; however, the pathway still remains active (Imam, Schäuble, Valenzuela, López García de Lomana, et al., 2015).

The cell synthesizes fatty acids which can be utilized in the cell or converted into lipid storage molecules (triacylglycerol). Beta oxidation breaks down fatty acids that have been previously synthesized by the algal cell. Future work needs to be completed in order to determine when fatty acid synthesis and beta oxidation are most active. Although it is known that under nitrogen limitation lipid storage increases, there is still uncertainty around the mechanisms of fatty acid synthesis and beta oxidation under nitrogen limited conditions in relation to lipid storage. Some believe that under nitrogen limitation, no fatty acid synthesis is occurring and the cell is utilizing already formed fatty acids to form lipid storage molecules such as triacylglycerol (Xiong et al., 2010).

Triacylglycerol (TAG) synthesis and degradation under different light conditions (photoautotrophic and heterotrophic growth) has shown conflicting results in metabolic reconstructions. Several metabolic reconstructions report an increase in flux for TAG synthesis (Imam, Schäuble, Valenzuela, López García de Lomana, et al., 2015; Vieler et al., 2012) while others report an increase in TAG synthesis flux when the algae cells are exposed to dark conditions (Wu et al., 2015; Zuñiga et al., 2018). Contrary to light intensity, when nitrogen is limited in the system, it has been concluded that TAG synthesis will increase in flux (Chang et al., 2011; Imam, Schäuble, Valenzuela, López García de Lomana, et al., 2015; Radakovits et al., 2012; Vieler et al., 2012). TAG degradation occurs when the cell no longer has access to an energy source such as light or organic carbon in the absence of light.

Similar to TAG synthesis and degradation, polyglucose (carbohydrate) synthesis and degradation has conflicting results when analyzing metabolic reconstructions under different light conditions. When light is present, it has been found that the synthesis of polyglucose increases (Juneja et al., 2016). However, other studies have shown that in the absence of light the synthesis of polyglucose increases (Gomes de Oliveira Dal'Molin et al., 2011; Zuñiga et al., 2018). When the algal system is under nitrogen deplete conditions, starch synthesis increases in flux (Imam, Schäuble, Valenzuela, López García de Lomana, et al., 2015; Juneja et al., 2016; Xiong et al.,

2010). In addition, similarly to TAG degradation, starch degradation occurs when the cell no long has access to an energy source such as light or organic carbon in the absence of light.

The gluconeogenesis pathway is roughly the reverse of the glycolysis pathway. The pathway is not very well understood in relation to the three conditions. It is believed that the gluconeogenesis pathway is activated during heterotrophic growth more than photoautotrophic growth (Gomes de Oliveira Dal'Molin et al., 2011). Also, under nitrogen starvation it is believed that gluconeogenesis is downregulated which is why more storage compounds are formed (Radakovits et al., 2012).

3.3 Enzyme conservation method. Within the sixteen metabolic pathways chosen to represent algae metabolism, which enzymes to include within the pathways also had to be considered. All enzymes participating in irreversible reactions were made sure to be included along with all enzymes requiring or producing energy. Even though there are more enzymes in an alga than in our model, such as the 1000+ enzymes included in some metabolic reconstructions, we chose to focus on the enzymes necessary for the pathways to function and complete the desired outcome (example = TAG storage). **Table 3.2** lists all of the metabolic pathways included in the metabolic reconstruction analysis along with the number of enzymes included for each enzymatic pathway. Sixty-nine enzymes were chosen to be represented across the 16 pathways in the algae model. It should be noted that some enzymes are a part of multiple metabolic pathways.

Table 3.2 Number of enzymes included in all 16 metabolic pathways considered

Metabolic Pathways	Number of Enzymes in Pathway
Glycolysis	10
Pentose phosphate pathway	7
Tricarboxylic acid (TCA) cycle	9
Photosynthesis	5
Calvin cycle	4
Photorespiration	10
Ammonia assimilation	2
Nitrate assimilation	2
Glyoxylate cycle	5
Beta oxidation	4
Fatty acid synthesis	4
Carbohydrate (starch) synthesis	3
Carbohydrate (starch) degradation	2
Triacylglycerol (lipid) synthesis	4
Triacylglycerol (lipid) degradation	1
Gluconeogenesis	12

Once the enzymes represented in the 16 metabolic pathways of the model were chosen, the conservation of enzymes among different algae species was analyzed to determine if all enzymes were present in the metabolic reconstruction data sets for different algae species **(figure 3.1).** Each enzyme considered for the study was looked for in the eleven metabolic reconstruction data sets to see if the enzyme was present. If the enzyme was present, it was marked as conserved in that data set for the specific algae species. A literature review for experimental evidence was also completed for enzymes that were not included in the metabolic reconstruction data sets but were believed to be present in microalgae metabolism. The pathways analyzed with experimental evidence include: ammonia assimilation, nitrate assimilation, carbohydrate synthesis, triacylglycerol synthesis, carbohydrate degradation, and triacylglycerol degradation. Several experiments were performed in various studies that showed enzymes are present in the algae even though they are not represented in the metabolic reconstruction for the given species (Blanc et al., 2010; Dong et al., 2013; Jia et al., 2015; Kilian, Benemann, Niyogi, & Vick, 2011; Li, 2014; Meuser et al., 2011; Shen, Yuan, Pei, & Mao, 2010; Shi, 2000). **Figure 3.1** shows the enzyme conservation results from examining eleven metabolic reconstruction data sets as well as conducting a literature review for experimental evidence. A complete list of enzyme abbreviations can be found in **table A.1**.

Figure 3.1 Enzyme conservation analysis of 11 metabolic reconstruction data sets and experimental evidence for 69 enzymes of interest in 16 metabolic pathways.
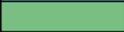
Key
- enzyme present
- enzyme with same function but different reaction present
- experimental evidence of enzyme presence
- missing or not identified enzyme

The metabolic pathways were well conserved among the various algae species. Nine of the sixteen pathways were completely conserved or had all of the enzymes present in the metabolic reconstruction data. These pathways include: glycolysis, photosynthesis, the Calvin cycle, nitrate assimilation, beta oxidation, fatty acid synthesis, starch synthesis, triacylglycerol synthesis, and starch degradation. For the additional seven metabolic pathways represented in the model, there were some differences among enzymes in the pathway for the various metabolic reconstructions. For example, in some species the enzyme was present in the algae species, but the enzymatic reaction shown for the enzyme in the metabolic reconstruction data set was different. For example, the enzyme fumarate reductase was originally included in the TCA cycle metabolic pathway, however after analyzing the data sets, it was found that succinate dehydrogenase was more common than fumarate reductase in the TCA cycle. Both succinate dehydrogenase and fumarate reductase have the same enzymatic reaction, but the enzymes have kinetic differences (Vieler et al., 2012; Cecchini, 2002). For the purpose of developing yield coefficients, the kinetic differences between the enzymes will not play a role and the enzyme included was assumed to be succinate dehydrogenase. However, for kinetic studies the enzyme difference should be analyzed further.

Besides having enzymes in the metabolic reconstructions with different reactions or kinetic parameters, some enzymes in the metabolic pathways were also missing completely. The enzymes could be missing because the reconstruction model did not consider analyzing a certain pathway, but also because the enzymes are not actually found in the algae species. The enzyme glucose-6-phosphatase was found missing among all of the algae species except one (*N. oceanica*). Glucose-6-phosphatase is the last enzyme in the gluconeogenesis pathway and is responsible for converting glucose-6-phosphate back to glucose. Reconverting back to glucose via gluconeogenesis is not necessary for the algal metabolism and it is preferable to remove the enzyme glucose-6-phosphatase from the model so that all glucose that accumulates in the algae cell cannot be secreted back into the medium and will be metabolized by the cell. Glucose-6-phosphatase is the one enzyme removed from the model and this is reflected by the fact that once glucose converts to glucose-6-phosphate by the enzyme glucokinase in the model it can no longer return to glucose.

Other enzymes (16 of the 69 enzymes considered) in the metabolic pathways are missing sporadically in just one of the seven species considered (see **Figure 3.1**). Even though one enzyme may be missing, it does not necessarily mean it is not present in the algae species. The

enzyme could have not been annotated for the metabolic reconstruction depending on the focus of the study utilizing the metabolic reconstruction data set such as the effects of varying light intensity or the effects on nutrient limitation. For example, photorespiration was one pathway in the *N. oceanica* metabolic reconstruction that was likely not included in the study because the focus of the work was on nutrient limitation and not the effect of oxygen saturation in the media, explaining why several enzymes are missing in the data set (Vieler et al., 2012). In addition, several metabolic reconstruction data sets were available for *C. reinhardtii* (Boyle & Morgan, 2009; Chang et al., 2011; Gomes de Oliveira Dal'Molin et al., 2011; Imam, Schäuble, Valenzuela, López García de Lomana, et al., 2015; Manichaikul et al., 2009). Among these metabolic reconstructions, some have an enzyme missing while others would have this enzyme included. Analyzing five metabolic reconstructions of the same species shows that there may be variance among the reconstruction data sets that does not accurately represent the enzymes in the algae species. Unfortunately, for all algae species beside *C. reinhardtii* only one metabolic reconstruction data set was available. In addition, the metabolic reconstructions are built off of genomic annotations, which could be fragmented and incomplete (Corteggiani Carpinelli et al., 2014). Metabolic reconstructions can also have gaps due to differences between generic and specific definitions of the same metabolites; naming and classification differences in databases can lead to holes in metabolic reconstructions (Krumholz et al., 2012). Additionally, when trying to balance large data sets for metabolic reconstructions to determine yield outputs, the removal of unbalanced equations in the reconstruction process can lead to additional gaps (Krumholz et al., 2012). Metabolic reconstruction data sets are not perfect representation of all the enzymatic properties in algae, but they are a valuable resource for understanding the metabolism of microalgae and the data sets give insight into shared enzymatic properties among multiple algae species.

When looking at all 69 enzymes considered, only four of the 69 enzymes are missing in two or more of the five species. 98% of enzymes are conserved in four out of the seven algae species and seventy-seven percent of enzymes are conserved in all seven algae species (**figure 3.2**). Such a low number of enzymes missing in two or more algae species shows the conservation of enzymes among different algae species.
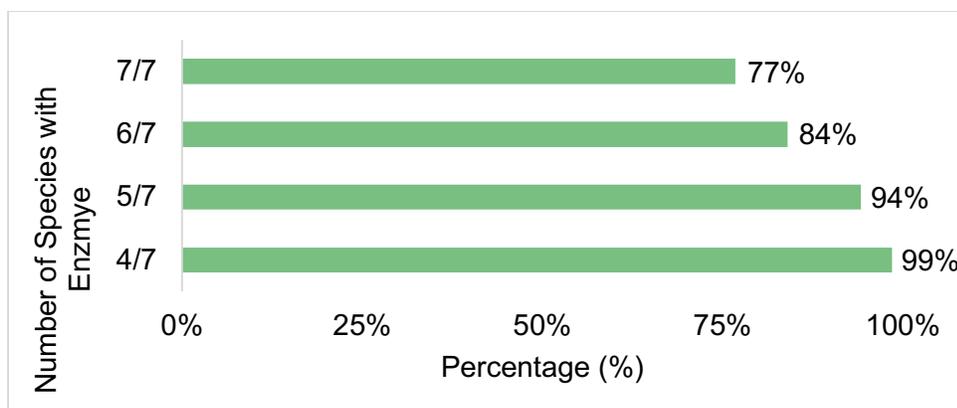
Figure 3.2 Percent of enzymes conserved in 4/7 to 7/7 algae species considered in the enzyme conservation analysis.

The majority of enzymes to be used for the development of a metabolic model are present in every algae species considered. This shows the conservation of pathways among algae species and how the model can be used for mixed algae communities. The conservation of enzymes found gives a strong basis for the simplification of metabolic data into simpler models based on key metabolites and lumped enzymatic reactions, known as a lumped pathway metabolic model. Boyle and Morgan took their metabolic reconstruction data set and solved for yield parameters following different variations of the same metabolic pathways within the cell. When different variations were used, the stoichiometric outputs of the metabolic reconstruction did not significantly vary (Boyle & Morgan, 2009). Little variation in stoichiometric properties based on changes in metabolic pathways gives a strong argument for the effectiveness of simplifying metabolic data and still achieving accurate and reproducible results. Although all of the enzymes, metabolites, and reactions in the cell preform a function, it is possible to shrink the reconstruction down in order to make the model manageable. By basing the lumped pathway metabolic model for mixed community algae wastewater treatment technologies off of metabolic reconstructions of specific algae species, we are able to harness complex enzymatic data and simplify the information to fit the needs of the wastewater processing modeling community (Baroukh et al., 2015; Daigger, 2011).

CHAPTER 4. Metabolic Model Development

4.1 Determination of Key Metabolites. The 69 enzymes used in the enzymatic conservation analysis are the necessary enzymes needed for the 16 pathways most prevalent in central carbon metabolism, nutrient assimilation, lipid synthesis, lipid storage, polyglucose synthesis and polyglucose storage. Understanding how key pathways of microalgal metabolism relate to one another is important. When building a lumped pathway metabolic model, the key metabolites of the model may be formed and/or consumed in multiple metabolic pathways. The interconnectedness of metabolic pathways requires a different framework for understanding the metabolic pathways and their relationships with one another. For example, ATP is formed and/or consumed across almost all pathways because all major metabolic pathways either use or produce energy. In addition, acetyl-CoA is a metabolite involved in seven metabolic pathways included in the model. The stoichiometric lumped pathway metabolic model for algal metabolism focuses on 14 metabolites that appear across the 16 metabolic pathways as shown in **table 4.1.**

Table 4.1 Metabolites Considered in Lumped Pathway Metabolic Model

Carbon dioxide	Acetate	Glucose
Glucose-6-phosphate	Glyceraldehyde-3-phosphate	Acetyl-CoA
Biomass precursor	Functional biomass	Triacylglycerol (Lipid)
Polyglucose (carbohydrate)	Ammonia	Nitrate
Nicotinamide adenine dinucleotide (NADH)	Adenosine triphosphate (ATP).	

The 14 metabolites included are a part of multiple metabolic pathways considered. There are several additional metabolites in the major metabolic pathways used for the model. The metabolites not included in the model are produced and/or consumed in one single metabolic pathway or are a pool metabolite that is assumed to have a constant concentration in the cell based on the metabolite's function. For example, Coenzyme-A (CoA) is attached to Acetyl-CoA, however CoA is not included in the lumped pathway metabolic model; acetyl-CoA is represented as having the same chemical formula as acetate. It is assumed that CoA is held at a constant concentration in the cell. Coenzyme-A is either attached to an acetate, forming Acetyl-CoA, or is detached and waiting to attach. Coenzyme-A is not formed or consumed by any of the metabolic pathways in the model; it just changes form by becoming attached or detached to additional

metabolites which is why it is considered a pool metabolite. NAD$^+$ and ADP are also pool metabolites; only NADH and ATP are included in the lumped pathway metabolic model.

4.2 Converting Metabolic Pathways to Reaction Pathways. Once the metabolites for the lumped pathway metabolic model were chosen, the diversion points needed to be decided in order to relate the reactions to one another in an effective way for lumped pathway metabolic modeling. Although the reactions were initially analyzed by the metabolic pathways that the reactions were a part of, these pathways would not work for developing the lumped pathway metabolic model. Since metabolites are involved in multiple metabolic pathways, the pathways need to be reorganized by when the chosen metabolites have the potential to diverge from one metabolic pathway to another. For example, in glycolysis glucose is converted to glucose-6-phosphate by the first enzyme in the pathway, hexokinase . Once glucose-6-phosphate is in the cell, it can continue through glycolysis, converting to fructose-6-phosphate, or glucose-6-phosphate can begin to be synthesized into polyglucose. Glucose-6-phosphate is a key metabolite chosen because of the possible diversion from glycolysis to polyglucose synthesis. The first enzymatic reaction of glycolysis makes up reaction pathway six in the lumped pathway metabolic model. In a similar manner, glycolysis was broken down into a total of three reaction pathways: glucose uptake into the cell (glucose to glucose-6-phosphate), conversion of glucose-6-phosphate to glyceraldehyde-3-phosphate, and the reaction converting glyceraldehyde-3-phosphate to pyruvate. This process was completed for all the metabolic pathways in order to convert the metabolic pathways into reaction pathways. A resulting 15 reaction pathways (represented by R1-R15) were developed for the 16 original metabolic pathways considered. Thirteen of the fifteen reaction pathways were formed directly from the enzymatic reactions involved in the formation and consumption of each key metabolite. The other two reaction pathways, biomass precursor formation reaction pathway and functional biomass formation pathway, were adapted from Guest et al., 2013. **Figure 4.1** shows all of the reaction pathways and their relationships to the metabolites in the lumped pathway metabolic model. The reaction pathways included in different metabolic processes and their function are described below.
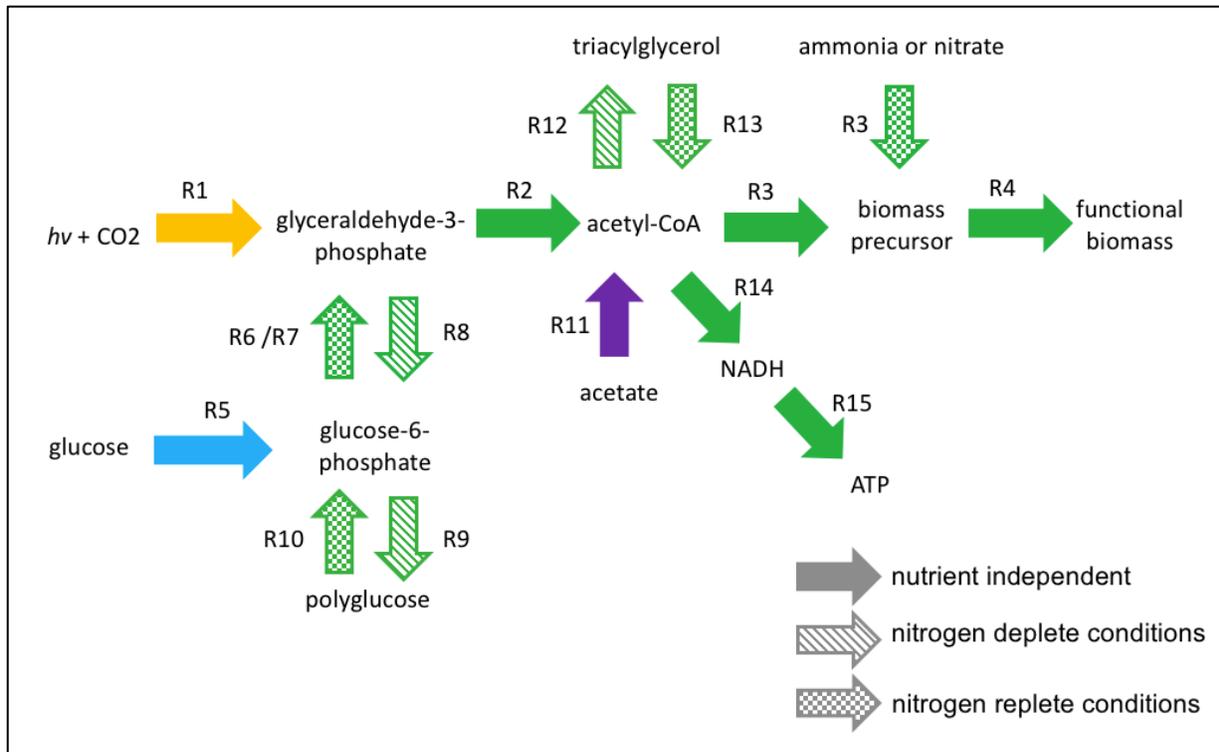
Figure 4.1 Schematic of lumped pathway metabolic model including all reaction equations for photoautotrophy and heterotrophy. Completely shaded arrows are active for all growth conditions, lined arrows are active of nitrogen deplete conditions only and checkered arrows are active for nitrogen replete conditions only. The yellow (R1), blue (R5), and purple arrows (R11) are only active one at a time for photoautotrophic growth, heterotrophic growth with glucose, and heterotrophic growth with acetate respectively.

4.2.1 Photoautotrophy. Photoautotrophy comprises photosynthetic processes in the algal metabolism, including the photosynthesis light reactions and the Calvin cycle, or dark reactions (R1). The cell uptakes carbon dioxide and the end products of the photoautotrophic process are glyceraldehyde-3-phosphate (G3P) and oxygen (Blankenship, 2014). The lumped pathway metabolic model assumed that there is sufficient light to support the photosynthetic process. The exact amount of light will need to be considered if the model is to be used for determining the rate of photoautotrophic processes in algae.

4.2.2 Heterotrophy. Heterotrophic growth is considered for carbon sources acetate (R11) and glucose (R5) in the lumped pathway metabolic model. Both acetate and glucose require one mole of ATP per mole of acetate or glucose transported into the cell. Acetate is then metabolized through the cell via the glyoxylate cycle and glucose is metabolized via the Embden-Meyerhof-Parnas (EMP) pathway (Nelson, Lehninger, & Cox, 2008).

4.2.3 Biopolymer Storage and Mobilization. Algae store carbon in the cell as carbohydrate and/or lipid biopolymers. The carbohydrate biopolymers are assumed to be stored in the form of polyglucose which is equivalent to starch. Polyglucose is formed during nutrient deplete conditions from glucose-6-phosphate. Energy in the form of ATP is also required for the storage of carbohydrates (R9). Under nutrient replete conditions, stored carbohydrates in the cell can be mobilized and used as a carbon source by breaking down polyglucose, without an energy input, into glucose-6-phosphate (R10) which can then undergo gluconeogenesis and form glyceraldehyde-3-phosphate used for cell growth (R6/R7) (Nelson et al., 2008).

The lipid biopolymers stored and mobilized by algae are assumed to be in the form of triacylglycerol (TAG) molecules for all algae species considered, although lipid biopolymers may be present in numerous forms. TAG is formed during nutrient deplete conditions from acetyl-CoA undergoing fatty acid synthesis to form palmitate and then further combining three palmitate molecules with a glycerol molecule to form TAG (R12) (Guest et al., 2013). Both steps require ATP in order to form and store TAG. The glycerol concentration within the algae is assumed to be constant and either in the attached form as a part of a TAG molecule, or as a detached glycerol-3-phosphate (similar to coenzyme-A). With nutrient replete conditions, TAG is mobilized in the cell and used as a carbon source in the form of acetyl-CoA for cell growth (R13). TAG mobilization requires energy to break down the TAG molecule back into the fatty acid components.

4.2.4 Biomass Production Nutrient Uptake and Nutrient Assimilation. Protein, DNA, and RNA synthesis are all necessary metabolic functions in the cell. These processes are lumped into two reaction equations adapted from Guest et al., 2013 and van Aalst-van Leeuwen, 1997. Biomass production is first represented by reaction pathway three (R3): acetyl-CoA forming biomass precursors, such as amino acids. Reaction pathway three balances catabolism of acetyl-CoA required for forming protein, DNA, and RNA precursors from acetyl-CoA (δ_X). Along with the formation of biomass precursors from acetyl-CoA, nitrogen and phosphorus assimilation into the cell are also considered a part of reaction three. The amount of energy in the form of ATP required to transport nutrients in the form of nitrate, ammonia, and phosphate are represented as δ_{NO}, δ_{NH}, and δ_{PO} respectively. The formation of biomass precursors also requires an amount of ATP, α_M. Biomass precursor polymerization to form functional biomass is represented by reaction pathway four. The amount of ATP required for functional biomass formation is represented by the amount of ATP required for polymerization, α_X, and the amount of ATP required for cellular maintenance, m_{ATP}. Both biomass precursor molecules and functional biomass molecules have the same

biomass composition, $CH_{1.8}O_{0.5}N_{0.2}P_{0.1}$ (Guest et al., 2013; Roels, 1980) in the lumped pathway metabolic model. Constant parameters descriptions and values can be found in **table A.2.**

4.2.5 Catabolism and Oxidative Phosphorylation. The tricarboxylic acid (TCA) cycle catabolizes acetyl-CoA for cellular energy production in the form of NADH (R14). NADH further undergoes oxidative phosphorylation to release oxygen from the cell and produce ATP that can be utilized by the cell for growth, storage, and maintenance processes (R15). Oxidative phosphorylation relies on the P/O ratio in the lumped pathway metabolic model to determine how much ATP is produced per mole of NADH oxidized. The P/O ratio, δ_{PO}, can vary with changes in the algal metabolism, however, the common modeling practice of holding the P/O ratio constant is used for the lumped pathway metabolic model (Roels, 1983; White, 2007). In addition, it has been shown that the P/O ratio does not vary with changes in carbon energy sources (carbon dioxide, acetate, and glucose) (Verduyn, Stouthamer, Scheffers, & Dijken, 1991).

4.3 Formation of Reaction Equations. The lumped enzymatic reactions making up each reaction pathway (R1-R15) in **figure 4.1** are converted to a c-mole basis for the lumped pathway metabolic model. A c-mole basis is used to compare the carbon flow throughout algal metabolism regardless of how many carbon atoms make up a given metabolite. Normalizing the metabolites to a c-mole basis allows for easier comparison and increased model capabilities (Roels, 1980, 1983; van Aalst-van Leeuwen, Pot, van Loosdrecht, & Heijnen, 1997b). **Table 4.2** below shows all of the reaction equations on a c-mole basis. The reaction equations are divided by the number of carbon moles that will make sure every metabolite in the reaction equation is on a c-mole basis. For example, if there is one glyceraldehyde-3-phosphate (three carbon molecule) in the reaction pathway equation, the glyceraldehyde-3-phosphate molecule wound need to be divided by three. However, if there were two glyceraldehyde-3-phosphate molecules formed in the reaction equation, the glyceraldehyde-3-phosphate metabolite would need to be divided by six for the six carbons present in the form of glyceraldehyde-3-phosphate. The entire reaction equation is divided by the same number so as not to change the relationship between the metabolites in the reaction. For further analysis, the reaction equations are set equal to zero by moving metabolites involved in the reaction pathway forming the reaction equation to one side of the equation. The reactants being consumed are subtracted metabolites and the products being formed are added metabolites.

Table 4.2 Reaction Equations Included in the Metabolic Model

Equation	Reaction	Stoichiometry	Citations
R_1	Synthesis of G3P from CO_2	$\alpha_P hv + CO_2 \rightarrow O_2 + \frac{1}{3}G3P$	[Caspi, Guest, Placzek]
R_2	Synthesis of acetyl-CoA from G3P	$\frac{1}{3}G3P \rightarrow \frac{2}{3}NADH + \frac{2}{3}ATP + \frac{1}{3}CO_2 + \frac{1}{3}acetylCoA$	[****]
R_3[a]	Synthesis of biomass precursors from acetyl-CoA	$\frac{1}{2}(1 + \delta_x + \delta_n)acetylCoA + cNH_3 + dPO_4^{3-}$ $+ \left(\alpha_m + d\epsilon - \frac{1}{2}\delta_n\right)ATP$ $\rightarrow CH_aO_bN_cP_d + (\delta_x + \delta_n)CO_2 + (2\delta_x - 0.1)^c NADH$	[Guest, Smolders, van Leeuwen]
R_4	Formation of functional biomass and cell maintenance	$CH_aO_bN_cP_d + \left(\alpha_x + \frac{m_{ATP}}{\mu_{max}}\right)ATP \rightarrow \frac{1}{n}(CH_{1.8}O_{0.5}N_{0.2}P_{0.1})_n$	[van Leeuwen, NDVY]
R_5	Glucose Transport	$\frac{1}{6}Glucose + \frac{1}{3}ATP \rightarrow \frac{1}{3}G6P$	[Tanner, Perez-Garcia]
R_6	Upper Glycolysis	$\frac{1}{6}G6P + \frac{1}{6}ATP \rightarrow \frac{1}{3}G3P$	[de Oliveira Dal'Molin, Perez-Garcia]
R_7	Upper Glycolysis via Pentose Phosphate Pathway	$\frac{1}{6}G6P \rightarrow \frac{1}{6}G3P + \frac{1}{2}CO_2 + NADH$	[de Oliveira Dal'Molin, Nelson, Perez-Garcia]
R_8	Gluconeogenesis: synthesis of G6P from G3P	$\frac{1}{3}G3P \rightarrow \frac{1}{6}G6P$	[Nelson]
R_9	Polyglucose Synthesis	$\frac{1}{6}(polyglucose)_n + \frac{1}{6}G6P + \frac{1}{6}ATP \rightarrow \frac{1}{6}(polyglucose)_{n+1}$	[de Oliveira Dal'Molin, Nelson]
R_{10}	Polyglucose Degradation	$\frac{1}{6}(polyglucose)_{n+1} \rightarrow \frac{1}{6}(polyglucose)_n + \frac{1}{6}G6P$	[Nelson]
R_{11}	Acetate Transport	$\frac{1}{2}acetate + \frac{1}{2}ATP \rightarrow \frac{1}{2}acetylCoA$	[Placzek]
R_{12}[b]	Triacylglycerol Synthesis	$\frac{25.5}{51}acetylCoA + \frac{24}{51}ATP + \frac{42}{51}NADH \rightarrow \frac{1}{51}TAG$	[Hu, Kanehisa, Nelson]
R_{13}	Triacylglycerol Degradation	$\frac{1}{51}TAG + \frac{3}{51}ATP \rightarrow \frac{25.5}{51}acetylCoA + \frac{35}{51}NADH$	[Nelson]
R_{14}	Tricarboxylic Acid Cycle: carbon catabolism	$\frac{1}{2}acetylCoA \rightarrow CO_2 + \frac{11}{6}NADH + \frac{1}{2}ATP$	[de Oliveira Dal'Molin, Kanehisa]
R_{15}	Oxidative Phosphorylation	$NADH + \frac{1}{2}O_2 \rightarrow \delta_{PO}ATP$	[Nelson, NDVY]

[a] In Reaction equation 3, NH_3 may be replaced with NO_3^-

[b] Elemental TAG composition is assumed to be $C_{51}H_{98}O_6$.

[c] $(2\delta_x - 0.1)$ is the simplified form of $\frac{4(1+\delta_x)-4.2}{2}$ where 4 is the oxidation value of carbon in the carbon source, 4.2 is the oxidation value of carbon in biomass, and 2 is the number of electrons retrieved per mole of NADH oxidized.

The fifteen reaction equations, normalized to a c-mole basis, used in the development of linear equations for the lumped pathway metabolic model. Constant parameters descriptions and values can be found in Table A.2

4.3.1 Growth Conditions Considered and Reaction Equations Active. Although there are 15 pathways in the lumped pathway metabolic model, the 15 pathways are not always active for every algae processing situation. **Table 4.3** shows the growth conditions considered and the corresponding reaction equations that are active for the given conditions. There is no one condition in which all of the reaction equations are present. The conditions that are varying include carbon source: carbon dioxide (photoautotrophic), acetate (heterotrophic), or glucose (heterotrophic) and the nitrogen source: ammonia (nutrient replete), nitrate (nutrient replete), or no nitrogen source (nutrient deplete). The reaction equations included for nutrient replete conditions with ammonia and nutrient replete conditions with nitrate are the same, however the coefficients used in the biomass precursor reaction equation, R3, will vary with respect to acetyl-CoA, carbon dioxide, and ATP based on the nitrogen source used.

Table 4.3 Reaction equations active for each growth and nutrient condition considered.

Conditions	Active Reactions Equations														
	1	2	3	4	5	6	7	8	9	10	11	12	13	14	15
Photoautotrophic Growth Nutrient Replete	X	X	X	X		X			X			X		X	X
Photoautotrophic Growth Nutrient Deplete	X	X	X	X			X			X			X	X	X
Heterotrophic Growth on Acetate Nutrient Replete		X	X	X			X	X	X		X	X		X	X
Heterotrophic Growth on Acetate Nutrient Deplete		X	X	X			X	X		X	X	X	X	X	X
Heterotrophic Growth on Glucose Nutrient Replete		X	X	X	X		X	X	X			X		X	X
Heterotrophic Growth on Glucose Nutrient Deplete		X	X	X	X		X	X		X			X	X	X
Mobilization of Storage Compounds Nutrient Replete		X	X	X			X	X	X			X		X	X

Based on the carbon source and growth conditions in the cell, certain reactions will be active under the given conditions; not all 15 reactions are active at any given time. For example, reaction one (R1) is only active under photoautotrophic growth. In addition, reaction pathways nine and twelve (R9: polyglucose synthesis and R12: triacylglycerol synthesis) are only active under nitrogen limited conditions. Reactions two through five (R2-R4) are active under all growth and media conditions. These reactions include: the second half of glycolysis (R2), acetyl-CoA to biomass precursors (R3), and biomass precursors to functional biomass (R4). These three reactions make up the core central metabolism pathway which can be seen from the straight path from R2-R4 in **figure 4.1.**

The tricarboxylic acid cycle (TCA cycle) and oxidative phosphorylation reactions equations, R14 and R15 respectively are also present under all growth and media conditions because the algal metabolism is always producing or consuming energy compounds, NADH and ATP. Depending on the carbon source considered for the growth conditions being tested, the reaction equations associated with carbon uptake and metabolism will vary. For photoautotrophic growth, photosynthesis (R1) will be included. For heterotrophic growth on acetate, acetate transport into the cell (R11) will be included. For heterotrophic growth on glucose, glucose transport into the cell (R5) and the first half of the glycolysis pathway (R6/R7) will be active and included in the set of linear equations.

In **figure 4.1**, it is shown that either reaction 6 (R6), the first half of glycolysis (glucose-6-phosphate to glyceraldehyde-3-phosphate) or reaction 7 (R7), the first half of glycolysis also including the pentose phosphate pathway, will be included in the set of active reactions equations for a given set of conditions. The pentose phosphate pathway is active under heterotrophic growth conditions and nitrogen limited growth conditions (Imam, 2015; Perez-Garcia, 2011). This includes all sets of reaction equations except for photoautotrophic growth in nutrient replete media. Gluconeogenesis (R8) is a reaction equation that acts in reverse of glycolysis and converts pyruvate back to glucose-6-phosphate. Gluconeogenesis is only present under heterotrophic growth conditions (Baroukh, Turon, & Bernard, 2017). Storage compound (polyglucose and triacylglycerol) synthesis and storage compound degradation are also active under different growth conditions; both synthesis and degradation of storage compounds cannot be active at the same time. Under nutrient replete conditions, polyglucose (PG) synthesis, R9, and triacylglycerol (TAG) synthesis, R12, are active reaction equations. Under nutrient deplete, or nutrient limited conditions, polyglucose degradation, R10, and triacylglycerol degradation, R13, are active reaction equations (Guest et al., 2013).

4.4 Forming Sets of Linear Equations for All of the Conditions Being Evaluated. To determine the rates at which specific metabolites are being formed, consumed, mobilized, or degraded for each condition set, a set of linear equations must be formed from the given reaction equations representing each condition. The linear equations are a set of equations that represent the rate of uptake, formation, consumption, degradation, or mobilization for each metabolite in the model. To form the linear equations for each metabolite, the reaction equations are inserted into a matrix that is multiplied by a rate vector. The matrix is x rows (for the number of reaction equations active for each condition as shown in **table 4.3**) by 16 columns (for the 16 metabolites

being considered. If a certain reaction equation does not have a given metabolite, then a zero is inserted into the matrix (Roels, 1983). The matrix is different for each condition; however, the number of columns never changes. The rate vector is 16 rows (for the sixteen metabolites present in the model) by 1 column. Each term in the rate vector is r_i where i is equal to one of the sixteen metabolites. Definitions for the rate equations can be found in **appendix A.3**. Multiplying the active reaction equations matrix by the rate vector will give a set of linear equations for each condition that represent the rate of uptake, formation, consumption, degradation, or mobilization for each metabolite. The linear equations are useful to understand all the reactions pathways each metabolite takes part in within the model.

4.4.1 Degree of Reduction Balance. The degree of reduction balance is an additional linear equation developed for each carbon source: carbon dioxide, acetate, and glucose in combination with each nitrogen source: ammonia and nitrate. To calculate the degree of reduction balance, the elemental matrix needs to be multiplied by the reaction rate vector and set equal to zero.

$$E * r = 0$$

The elemental matrix, E, is 4 rows by 16 columns. The four rows are for each element being tracked in the model: carbon, hydrogen, oxygen, nitrogen and the 14 columns represent the 14 metabolites in the metabolic model. The reaction rate matrix, r, is 14 rows by 1 column. The fourteen rows represent the reaction rate associated with each metabolite in the model. The degree of reduction balance is a c-mole based linear equation, therefore each reaction rate in the r column vector is multiplied by the number of carbon atoms in each metabolite. All of the metabolites that do not accumulate in the cell are set equal to zero. The non-zero reaction rates in the model are for the following metabolites: the carbon source being used (carbon dioxide, acetate, or glucose), functional biomass, polyglucose, triacylglycerol, and oxygen. Solving the matrix multiplication will result in the degree of reduction balance (Roels, 1983; Nielson, 1995).

The degree of reduction balance is used to show the transfer and demand of electrons by metabolites with non-zero reaction rates in the model. The rate of electrons liberated is set equal to the rate of electron sinks, or electron demand. The reaction rate for oxygen (electrons liberated) is represented on one side of the balance and is set equal to the sum of all of the other reaction rates terms for the model and their corresponding coefficients (electron sinks).

Phosphorus transport and accumulation is included in the model; however, phosphorus is not included in the degree of reduction balance linear equation. Phosphorus is not included because the degree of reduction balance is used to show the transfer of electrons among metabolites and phosphorus is only considered to stay in one state, as orthophosphate that is then assimilated into cell biomass. Also, the elemental phosphate in metabolites is not considered for the lumped pathway metabolic model which is representing all metabolites on a c-mole basis; only the energy involved in phosphate uptake is considered (in reaction equation R3).

Table 4.4 Linear equations for photoautotrophic nutrient-replete metabolism

#	Equation	Units
1[a]	$r_{NADH} = 0 = \frac{35}{51}r_{13} + \frac{11}{6}r_{14} - r_{15} + \frac{2}{3}r_2 + r_3(-0.1 + 2\delta_x)$	$moles - (NADH) - hour^{-1}$
2	$r_{ATP} = 0 = -\frac{1}{17}r_{13} + \frac{1}{2}r_{14} + \delta_{PO}r_{15} + \frac{2}{3}r_2 - \frac{1}{6}r_6$ $- \left(\alpha_x + \frac{m_{ATP}}{\mu_{max}}\right)r_4 + (-\alpha_M - 0.1\epsilon + \frac{1}{2}\delta_n)r_3$	$moles - (ATP) - hour^{-1}$
3	$r_{G6P} = 0 = r_{10} - r_6$	$moles - (G6P\ as\ C) - hour^{-1}$
4	$r_{G3P} = 0 = r_1 - r_2 + r_6$	$moles - (G3P\ as\ C) - hour^{-1}$
5	$r_{ACoA} = 0 = r_{13} - r_{14} + \frac{2}{3}r_2 - r_3(1 + \delta_n + \delta_x)$	$moles - (ACoA\ as\ C) - hour^{-1}$
6	$r_{X_{pre}} = 0 = r_3 - r_4$	$moles - (X_{pre}\ as\ C) - hour^{-1}$
7	$r_{X_{alg}} = r_4$	$moles - (X_{alg}\ as\ C) - hour^{-1}$
8	$r_{TAG} = -r_{13}$	$moles - (TAG\ as\ C) - hour^{-1}$
9	$r_{PG} = -r_{10}$	$moles - (PG\ as\ C) - hour^{-1}$
10	$r_{O_2} = r_1 - \frac{1}{2}r_{15}$	$moles - (O_2) - hour^{-1}$
11	$r_{CO_2} = -r_1 + r_{14} + \frac{1}{3}r_2 + (\delta_n + \delta_x)r_3$	$moles - (CO_2\ as\ C) - hour^{-1}$
12[b]	$4r_{O_2} = \frac{290}{51}r_{TAG} + 4r_{PG} + 4.2r_{X_{alg}}$	-

[a] Assumes $FADH_2 = \frac{2}{3}NADH$ and $NADH_2 = NADH$

[b] Degree of Reduction balance based on Roels, 1983 and Nielsen, 1995. In #12, the coefficient for r_{Xalg} is 5.8 when nitrate is the nitrogen source.

Table 4.4 shows an example of the linear equations and degree of reduction balance for photoautotrophic nutrient replete metabolism. The list of abbreviation for the reaction equations can be found in **appendix A.3**. The additional linear equations and degree of reduction balances associated with the given growth conditions can be found in **appendix A.4 – A.10**.

4.4.2 Determination of Specific Rates from Linear Equations. Although each metabolite has a linear equation, they are not all useful in determining the rate equations and stoichiometric coefficients alone because there are too many unknown values. Solving a set of linear equations

for a given metabolite rate allows for the model to be simplified and provide useful information about algae metabolism. Using the set of linear equations for a given growth and nutrient condition as well as the degree of reduction balance for the given carbon source, the specific rate of metabolites can be determined. To solve the sets of linear equations, all metabolites which do not enter, or become stored in the cell are set equal to zero. These linear equations are the same regardless of growth condition and include: r_{ACoA}, r_{G6P}, r_{G3P}, $r_{X_{pre}}$, r_{NADH}, and r_{ATP}. Once the selected metabolite equations are set equal to zero, the sets of linear equations were solved. **Table 4.5** shows an example of the solved linear equations for nutrient replete photoautotrophic metabolism. Additional linear equation solutions can be found in **appendix A.11 – A.13**.

Table 4.5 Linear equation solutions for photoautotrophic nutrient-replete metabolism

Description [units]	Nutrient-Replete Metabolism	Nutrient-Deplete Metabolism
Specific Rate of Photosynthesis [moles-(CO_2 fixed to G3P)·moles-(X_{alg} as C)$^{-1}$·hour^{-1}]	$q_{PHOT}^{NR} = \dfrac{\mu^{NR}}{Y_{X_{alg}}^{NR}} + \dfrac{q_{PG}^{NR}}{Y_{PG}^{NR}} + \dfrac{q_{TAG}^{NR}}{Y_{TAG}^{NR}} + \dfrac{m_{ATP}^{NR}}{Y_{ATP}^{NR}}$	$q_{PHOT}^{ND} = \dfrac{\mu^{ND}}{Y_{X_{alg}}^{ND}} + \dfrac{q_{PG}^{ND}}{Y_{PG}^{ND}} + \dfrac{q_{TAG}^{ND}}{Y_{TAG}^{ND}} + \dfrac{m_{ATP}^{ND}}{Y_{ATP}^{ND}}$
Specific Rate of CO_2 Production [moles-(CO_2)·moles-(X_{alg} as C)$^{-1}$·hour^{-1}]	$q_{CO_2}^{NR} = -q_{PG}^{NR} - q_{TAG}^{NR} - \mu^{NR}$	$q_{CO_2}^{ND} = -q_{PG}^{ND} - q_{TAG}^{ND} - \mu^{ND}$
Specific Rate of O_2 Production [moles-(O_2)·moles-(X_{alg} as C)$^{-1}$·hour^{-1}]	$q_{O_2}^{NH} = q_{PG}^{NH} + \frac{145}{102}q_{TAG}^{NH} + \frac{21}{20}\mu^{NH}$ $q_{O_2}^{NO} = q_{PG}^{NO} + \frac{145}{102}q_{TAG}^{NO} + \frac{29}{20}\mu^{NO}$	$q_{O_2}^{ND} = q_{PG}^{ND} + \frac{145}{102}q_{TAG}^{ND} + \frac{21}{20}\mu^{ND}$

Note on superscripts: NH; ammonia as nitrogen source, NO; nitrate as nitrogen source, NR; nitrogen source present, could be ammonia or nitrate, ND; no nitrogen source present

Note on parameters: Specific rate equations described using parameter q (specific rate of production), Y (yield coefficient), and μ (functional biomass growth rate)

q_{PHOT}; specific rate of CO_2 fixation to G3P, moles-(G3P as C)·mole-(X_{alg} as C)$^{-1}$·hr^{-1}

q_{CO2}; specific rate of CO_2 production, moles-(CO_2)·mole-(X_{alg} as C)$^{-1}$·hr^{-1}

q_{O2}; specific rate of O_2 production, moles-(O_2)·mole-(X_{alg} as C)$^{-1}$·hr^{-1}

The linear equations are solved for three rate equations relevant to cell growth: the specific rate of the carbon source fixed in the cell (carbon dioxide, acetate, or glucose), the specific rate of carbon dioxide production, and the specific rate of oxygen production. The specific rates are developed from the enzymatic reactions and metabolic properties in algae under different growth conditions to have robust parameters in order to ground the derivation of more complex kinetic parameters in intrinsic biochemical properties of the cell. The scope of this work did not develop additional kinetic properties, but the linear equation solutions developed could be used to do so.

4.4.3 Determination of Stoichiometric Yield Coefficients from Linear Equations. In addition to the linear equation solutions, the set of linear equations for a given condition can also be used

to solve for stoichiometric yield coefficients. Stoichiometric yield coefficients were solved for four metabolites: polyglucose (carbohydrates), triacylglycerol (lipid), biomass, and ATP. The stoichiometric coefficients were solved for with the units of c-moles of metabolite of interest (one of the four previously listed) per c-mole of carbon source fixed in the cell. The carbon source fixed within in the cell is based on the growth condition being analyzed. Three carbon sources were considered for stoichiometric yield coefficient development: carbon dioxide (c-mole of carbon dioxide fixed to c-mole of glyceraldehyde-3-phosphate), acetate (c-mole acetate fixed to c-mole acetyl-CoA), and glucose (c-mole glucose fixed to c-mole glucose-6-phosphate). **Table 4.6** shows the stoichiometric yield coefficients for photoautotrophic metabolism (nutrient replete and deplete). Additional stoichiometric yield coefficients for heterotrophic growth (acetate and glucose) can be found in **appendix A.14 – A.16**.

Table 4.6 Stoichiometric yields for photoautotrophic metabolism

Description [units]	Nutrient-Replete Metabolism	Nutrient-Deplete Metabolism
yield of polyglucose on CO_2 fixed to G3P [(C-moles PG)·(C-mole CO_2 fixed to G3P)$^{-1}$]	$Y_{\frac{NR}{PG}} = \dfrac{18 + 34\delta_{PO}}{15 + 34\delta_{PO}}$	$Y_{\frac{ND}{PG}} = \dfrac{18 + 34\delta_{PO}}{12 + 35\delta_{PO}}$
yield of lipid on CO_2 fixed to G3P [(C-moles LI)·(C-mole CO_2 fixed to G3P)$^{-1}$]	$Y_{\frac{NR}{LI}} = \dfrac{306 + 578\delta_{PO}}{135 + 771\delta_{PO}}$	$Y_{\frac{ND}{LI}} = \dfrac{306 + 578\delta_{PO}}{297 + 813\delta_{PO}}$
yield of biomass on CO_2 fixed to G3P [(C-moles biomass)·(C-mole CO_2 fixed to G3P)$^{-1}$][a]	$Y_{X_{alg}}$ $= \dfrac{170\delta_{PO} + 90}{90\alpha_M + 90\alpha_x + 90(0.1\epsilon) + 174\delta_{PO} + 165\delta_N\delta_{PO} + 45\delta_x - 15\delta_{PO}\delta_x + 45}$	
yield of ATP on CO_2 fixed to G3P [(moles of ATP)·(C-mole CO_2 fixed to G3P)$^{-1}$]	$Y_{\frac{NR}{ATP}} = \dfrac{9 + 17\delta_{PO}}{9}$	$Y_{\frac{NR}{ATP}} = \dfrac{9 + 17\delta_{PO}}{9}$

[a] Yield of biomass can only happen under nutrient replete conditions

Polyglucose and triacylglycerol stoichiometric coefficients were solved for because of the interest in carbohydrates and lipids for bio-based products, such as biofuels (Pittman, Dean, & Osundeko, 2011). In addition, carbohydrate and lipid storage play a role in nutrient uptake in the absence of sunlight and an external carbon source during phototrophic growth; the storage molecules allow for the uptake of nutrients by algae cells at night time, or when it is dark which is a major benefit to the wastewater treatment industry (Gardner-Dale, Bradley, & Guest, 2017). Biomass growth is important to track in order to know how much biomass will need to be removed from the wastewater treatment system so that the system can continue at optimal function. The biomass removed can be used in multiple ways. The algae can be anaerobically digested for energy or the biomass can be harnessed for multiple bio-products such as biofuel feedstock or fertilizer (Benemann, 1979; Skjånes, Rebours, & Lindblad, 2013; Ward, Lewis, & Green, 2014). ATP stoichiometric coefficients are important values to know because ATP is the energy source of the cell; without ATP, cell growth, maintenance, and nutrient uptake would not function properly, and algae could not be used to treat wastewater.

CHAPTER 5. Conclusion and Engineering Significance

5.1 Conclusion. When considering **table 4.6**, it can be seen that many of the developed yield coefficients are only dependent on one parameter, δ_{PO}, or the constant P/O ratio. For photoautotrophic metabolism, six out of the seven stoichiometric yield coefficients are solely based on the P/O ratio after the systems of linear equations are solved. A similar trend is observed for the other conditions with a total of eighteen out of twenty-one developed stoichiometric yield coefficients being based solely on δ_{PO}. In addition, δ_{PO} is a parameter grounded in the biochemical processes involved in oxidative phosphorylation. In algae metabolism, along with most microbial metabolisms, δ_{PO} is a fixed ratio that can only vary from one to three moles of ATP produced per mole of NADH oxidized (White, 2007). This range is based on transport properties and the structure of the ATP synthase molecule involved in oxidative phosphorylation (White, 2007). In the model development, δ_{PO} is assumed to be equal to two moles of ATP produced per mole of NADH oxidized and the biochemical restriction show that the uncertainty surrounding this parameter is minor since the value can only vary from one to three (Stouthamer, 1973a). Having a majority of the developed stoichiometric coefficients rely on one processing parameter, δ_{PO}, that has little uncertainty surrounding its value allows for more robust modeling processing parameters that are grounded in biochemical mechanisms essential to algal metabolism. **Tables 5.1, 5.2, and 5.3** show the numerical yield coefficients for photoautotrophic growth, heterotrophic growth with acetate, and heterotrophic growth with glucose respectively based on solving the stoichiometric solutions (**appendix A.14 – A1.6**) with constant values given in **appendix A.2.**

Table 5.1 Stoichiometric yields for photoautotrophic metabolism

Description [units]	Nutrient-Replete with Ammonia	Nutrient-Replete with Nitrate	Nutrient-Deplete Metabolism
yield of polyglucose on CO_2 fixed to G3P [(C-moles PG)·(C-mole CO_2 fixed to G3P)$^{-1}$]	$Y_{\frac{NR}{PG}} = 1.036$	$Y_{\frac{NR}{PG}} = 1.036$	$Y_{\frac{ND}{PG}} = 1.049$
yield of lipid on CO_2 fixed to G3P [(C-moles LI)·(C-mole CO_2 fixed to G3P)$^{-1}$]	$Y_{\frac{NR}{LI}} = 0.872$	$Y_{\frac{NR}{LI}} = 0.872$	$Y_{\frac{ND}{LI}} = 0.760$
yield of biomass on CO_2 fixed to G3P [(C-moles biomass)·(C-mole CO_2 fixed to G3P)$^{-1}$]	$Y_{X_{alg\_NH}} = 0.726$	$Y_{X_{alg\_NO}} = 0.528$	NA[a]
yield of ATP on CO_2 fixed to G3P [(moles of ATP)·(C-mole CO_2 fixed to G3P)$^{-1}$]	$Y_{\frac{NR}{ATP}} = 4.778$	$Y_{\frac{NR}{ATP}} = 4.778$	$Y_{\frac{ND}{ATP}} = 4.778$

[a] Yield of biomass can only happen under nutrient replete conditions

Table 5.2 Stoichiometric for heterotrophic metabolism with acetate

Description [units]	Nutrient-Replete with Ammonia	Nutrient-Replete with Nitrate	Nutrient-Deplete Metabolism
yield of polyglucose on glucose fixed to G6P [(C-moles PG)·(C-mole glucose fixed to G6))$^{-1}$]	$Y_{\frac{NR}{PG}} = 0.625$	$Y_{\frac{NR}{PG}} = 0.625$	$Y_{\frac{ND}{PG}} = 0.600$
yield of lipid on glucose fixed to G6P [(C-moles LI)·(C-mole glucose fixed to G6P)$^{-1}$]	$Y_{\frac{NR}{LI}} = 0.777$	$Y_{\frac{NR}{LI}} = 0.777$	$Y_{\frac{ND}{LI}} = 0.502$
yield of biomass on glucose fixed to G6P [(C-moles biomass)·(C-mole glucose fixed to G6P)$^{-1}$][a]	$Y_{X_{alg\_NH}} = 0.490$	$Y_{X_{alg\_NO}} = 0.373$	NA[a]
yield of ATP on glucose fixed to G6P [(moles of ATP)·(C-mole glucose fixed to G6P)$^{-1}$]	$Y_{\frac{NR}{ATP}} = 2.500$	$Y_{\frac{NR}{ATP}} = 2.500$	$Y_{\frac{ND}{ATP}} = 2.500$

[a] Yield of biomass can only happen under nutrient replete conditions

Table 5.3 Stoichiometric yields for heterotrophic metabolism with glucose

Description [units]	Nutrient-Replete with Ammonia	Nutrient-Replete with Nitrate	Nutrient-Deplete Metabolism
yield of polyglucose on acetate fixed to acetyl-CoA [(C-moles PG)·(C-mole acetate fixed to acetyl-CoA)$^{-1}$]	$Y_{\frac{NR}{PG}} = 0.667$	$Y_{\frac{NR}{PG}} = 0.667$	$Y_{\frac{ND}{PG}} = 0.880$
yield of lipid on acetate fixed to acetyl-CoA [(C-moles LI)·(C-mole acetate fixed to acetyl-CoA)$^{-1}$]	$Y_{\frac{NR}{LI}} = 1.140$	$Y_{\frac{NR}{LI}} = 1.140$	$Y_{\frac{ND}{LI}} = 0.736$
yield of biomass on acetate fixed to acetyl-CoA [(C-moles biomass)·(C-mole acetate fixed to acetyl-CoA)$^{-1}$][a]	$Y_{X_{alg\_NH}} = 0.718$	$Y_{X_{alg\_NO}} = 0.547$	NA[a]
yield of ATP on acetate fixed to acetyl-CoA [(moles of ATP)·(C-mole acetate fixed to acetyl-CoA)$^{-1}$]	$Y_{\frac{NR}{ATP}} = 3.667$	$Y_{\frac{NR}{ATP}} = 3.667$	$Y_{\frac{ND}{ATP}} = 3.667$

[a] Yield of biomass can only happen under nutrient replete conditions

When analyzing the numerical solution of the stoichiometric yield coefficients, several trends can be observed. For example, the nitrogen replete source (ammonia or nitrate) only affects the growth yield coefficient parameters; the yield coefficients for polyglucose, lipid, and ATP are the same for if nitrogen is present in either form, ammonia or nitrate. The numerical solutions for biomass show that the nitrogen source ammonia is preferred for cells over nitrate and this is consistent with experimental data (Tchobanoglous et al., 2003). Ammonia is already in the correct reduction state when it enters the algal cell while nitrate must be reduced in order to be assimilated into algal biomass which requires more energy and leads to a lower biomass yield (Lewin, c1962). When considering the yield of polyglucose and lipid for all of the growth conditions, there are differences between the nitrogen replete and nitrogen deplete conditions. When nitrogen is not present, storage compounds such as polyglucose and lipids accumulate in the cell (Boyle & Morgan, 2009). The differences in values are caused primarily by the differences in energy requirements the cell needs to uptake and metabolize a given carbon source under different growth conditions and nutrient availability. It is also observed that ATP production in the cell is not based on nitrogen availability. For any given condition, the amount of ATP produced will be the same regardless if nitrogen is available to the cell or not. The amount ATP produce per c-mole of carbon fixed is the highest for photoautotrophic metabolism, which is consistent with other metabolic models finding and experimental evidence (Boyle & Morgan, 2009; Gomes de Oliveira Dal'Molin et al., 2011; Wágner et al., 2016; Zuñiga et al., 2018).

Stoichiometric yield coefficient results were compared with available stoichiometric yield coefficients reported in algae metabolic models for photoautotrophic growth (Al Ketife, Judd, &

Znad, 2016; Bello, Ranganathan, & Brennan, 2017; Buhr & Miller, 1983; Decostere et al., 2017, 2013; Juneja & Murthy, 2018; Murphy & Berberoglu, 2014; Park & Li, 2015; J. Yang et al., 2011). **Figure 5.1** shows the range of reported values found for grams of biomass produced per gram of carbon dioxide utilized. The numerical yield stoichiometric value is reported (with nitrate as nitrogen source) along with the range of biomass growth under photoautotrophic conditions with the possible range of δ_{PO} from one to three. It can be seen that the developed stoichiometric yield coefficient from this study for photoautotrophic biomass falls within the range of other algae model study's reported yield coefficients for photoautotrophic growth.
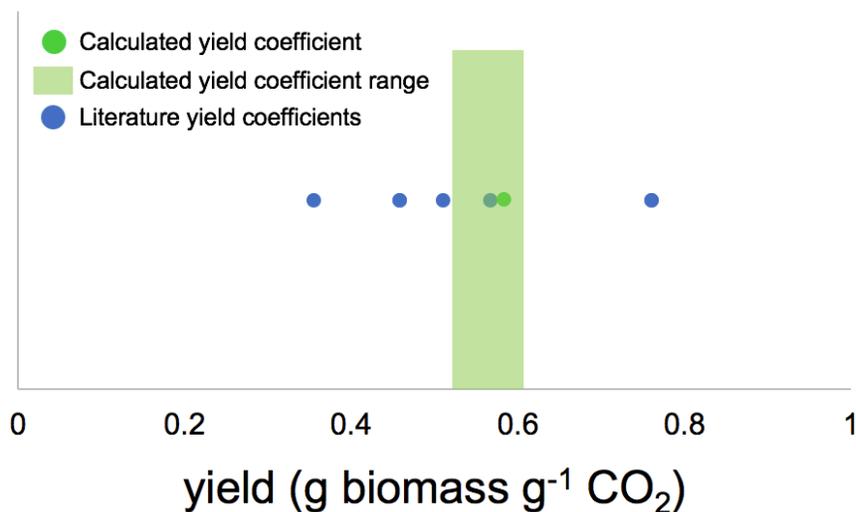
Figure 5.1 Comparison of photoautotrophic nutrient replete with nitrate biomass yield coefficient with photoautotrophic yield coefficients provided in literature. The range of the developed photoautotrophic yield coefficient with δ_{PO} varying from one to three moles of ATP produced per mole of NADH oxidized is also shown.

5.2 Engineering Significance. Establishing universal yield coefficients based on conserved metabolic properties of algae species will help advance the use of algal technologies in the wastewater treatment industry. A generalizable understanding of universally conserved metabolic properties under various growth conditions for algal species (i.e., photoautotrophic and heterotrophic) will lead to improved models for algae cultivation and support the adoption of algal technologies for biological nutrient removal in wastewater.

With improved models, algae technologies can be implemented more widely and operated more efficiently to improve WRRFs effluent quality. Water resource recovery facilities are located all around the world in different climates, temperature, and elevations. The variability in location can

change the communities of algae species that are grown in the area. Unfortunately, WRRFs do not have the resources to experimentally validate yield coefficients for each location. Having stoichiometric yield coefficients that do not rely on variation in external factors (temperature, pH, alkalinity, etc.) and are based on conserved metabolic properties will allow algae technologies at various WRRFs have robust models with limited uncertainty estimating the algae system's properties. In addition, the wastewater treatment community has developed a modeling platform in order to increase uniformity and ease modeling communication across the industry. Following this format in the development and presentation of the newly developed stoichiometric yield coefficients will also improve implementation of algae technologies into current modeling formats. WRRFs will be able to understand easily how algae system models operate similarly to current technologies at WRRFs which will promote adaptability of algae technologies.

REFERENCES

Adesanya, V. O., Davey, M. P., Scott, S. A., & Smith, A. G. (2014). Kinetic modelling of growth and storage molecule production in microalgae under mixotrophic and autotrophic conditions. *Bioresource Technology*, *157*, 293–304. https://doi.org/10.1016/j.biortech.2014.01.032

Al Ketife, A. M. D., Judd, S., & Znad, H. (2016). A mathematical model for carbon fixation and nutrient removal by an algal photobioreactor. *Chemical Engineering Science*, *153*, 354–362. https://doi.org/10.1016/j.ces.2016.07.042

Arnold, A., & Nikoloski, Z. (2013). Comprehensive classification and perspective for modelling photorespiratory metabolism. *Plant Biology*, *15*(4), 667–675. https://doi.org/10.1111/j.1438-8677.2012.00708.x

Balaji, S., Gopi, K., & Muthuvelan, B. (2013). A review on production of poly β hydroxybutyrates from cyanobacteria for the production of bio plastics. *Algal Research*, *2*(3), 278–285. https://doi.org/10.1016/j.algal.2013.03.002

Baroukh, C., Muñoz-Tamayo, R., Steyer, J.-P., & Bernard, O. (2014). DRUM: A New Framework for Metabolic Modeling under Non-Balanced Growth. Application to the Carbon Metabolism of Unicellular Microalgae. *PLOS ONE*, *9*(8), e104499. https://doi.org/10.1371/journal.pone.0104499

Baroukh, C., Muñoz-Tamayo, R., Steyer, J.-P., & Bernard, O. (2015). A state of the art of metabolic networks of unicellular microalgae and cyanobacteria for biofuel production. *Metabolic Engineering*, *30*, 49–60. https://doi.org/10.1016/j.ymben.2015.03.019

Baroukh, C., Turon, V., & Bernard, O. (2017). Dynamic metabolic modeling of heterotrophic and mixotrophic microalgal growth on fermentative wastes. *PLOS Computational Biology*, *13*(6), e1005590. https://doi.org/10.1371/journal.pcbi.1005590

Bello, M., Ranganathan, P., & Brennan, F. (2017). Dynamic modelling of microalgae cultivation process in high rate algal wastewater pond. *Algal Research*, *24*, 457–466. https://doi.org/10.1016/j.algal.2016.10.016

Benemann, J. R. (1979). Production of nitrogen fertilizer with nitrogen-fixing blue - green algae. *Enzyme and Microbial Technology*, *1*(2), 83–90. https://doi.org/10.1016/0141-0229(79)90103-0

Blanc, G., Duncan, G., Agarkova, I., Borodovsky, M., Gurnon, J., Kuo, A., … Etten, J. L. V. (2010). The Chlorella variabilis NC64A Genome Reveals Adaptation to Photosymbiosis, Coevolution with

Viruses, and Cryptic Sex. *The Plant Cell*, *22*(9), 2943–2955.

https://doi.org/10.1105/tpc.110.076406

Blankenship, R. E. (2014). *Molecular Mechanisms of Photosynthesis*. John Wiley & Sons.

Boyle, N. R., & Morgan, J. A. (2009). Flux balance analysis of primary metabolism in Chlamydomonas

reinhardtii. *BMC Systems Biology*, *3*(1), 4. https://doi.org/10.1186/1752-0509-3-4

Buchanan, B. B., Gruissem, W., Jones, R. L., & Vickers, K. (2015). *Biochemistry and Molecular Biology of

Plants*. Hoboken, UNITED KINGDOM: John Wiley & Sons, Incorporated. Retrieved from

http://ebookcentral.proquest.com/lib/uiuc/detail.action?docID=4035886

Buhr, H. O., & Miller, S. B. (1983). A dynamic model of the high-rate algal-bacterial wastewater

treatment pond. *Water Research*, *17*(1), 29–37. https://doi.org/10.1016/0043-1354(83)90283-X

Carey, R. O., & Migliaccio, K. W. (2009). Contribution of Wastewater Treatment Plant Effluents to

Nutrient Dynamics in Aquatic Systems: A Review. *Environmental Management*, *44*(2), 205–217.

https://doi.org/10.1007/s00267-009-9309-5

Carrier, G., Baroukh, C., Rouxel, C., Duboscq-Bidot, L., Schreiber, N., & Bougaran, G. (2018). Draft

genomes and phenotypic characterization of Tisochrysis lutea strains. Toward the production of

domesticated strains with high added value. *Algal Research*, *29*, 1–11.

https://doi.org/10.1016/j.algal.2017.10.017

Chang, R. L., Ghamsari, L., Manichaikul, A., Hom, E. F. Y., Balaji, S., Fu, W., … Papin, J. A. (2011).

Metabolic network reconstruction of Chlamydomonas offers insight into light-driven algal

metabolism. *Molecular Systems Biology*, *7*(1), 518. https://doi.org/10.1038/msb.2011.52

Chislock, M. F. (n.d.). Eutrophication: Causes, Consequences, and Controls in Aquatic c Ecosystems, 8.

Chisti, Y. (2008). Biodiesel from microalgae beats bioethanol. *Trends in Biotechnology*, *26*(3), 126–131.

https://doi.org/10.1016/j.tibtech.2007.12.002

Conley, D. J., Paerl, H. W., Howarth, R. W., Boesch, D. F., Seitzinger, S. P., Havens, K. E., … Likens, G. E.

(2009). ECOLOGY: Controlling Eutrophication: Nitrogen and Phosphorus. *Science*, *323*(5917),

1014–1015. https://doi.org/10.1126/science.1167755

Corteggiani Carpinelli, E., Telatin, A., Vitulo, N., Forcato, C., D'Angelo, M., Schiavon, R., … Valle, G.

(2014). Chromosome Scale Genome Assembly and Transcriptome Profiling of Nannochloropsis

gaditana in Nitrogen Depletion. *Molecular Plant*, *7*(2), 323–335.

https://doi.org/10.1093/mp/sst120

Daigger, G. T. (2011). A practitioner's perspective on the uses and future developments for wastewater treatment modelling. *Water Science and Technology*, *63*(3), 516–526. https://doi.org/10.2166/wst.2011.252

Decostere, B., Alvarado, A., Sánchez, E. M., Pauta, G. C., Rousseau, D. P., Nopens, I., & Hulle, S. W. V. (2017). Model based analysis of the growth kinetics of microalgal species residing in a waste stabilization pond. *Journal of Chemical Technology & Biotechnology*, *92*(6), 1362–1369. https://doi.org/10.1002/jctb.5131

Decostere, B., Janssens, N., Alvarado, A., Maere, T., Goethals, P., Van Hulle, S. W. H., & Nopens, I. (2013). A combined respirometer–titrimeter for the determination of microalgae kinetics: Experimental data collection and modelling. *Chemical Engineering Journal*, *222*, 85–93. https://doi.org/10.1016/j.cej.2013.01.103

Dong, H.-P., Williams, E., Wang, D., Xie, Z.-X., Hsia, R., Jenck, A., … Place, A. R. (2013). Responses of Nannochloropsis oceanica IMET1 to Long-Term Nitrogen Starvation and Recovery. *Plant Physiology*, *162*(2), 1110–1126. https://doi.org/10.1104/pp.113.214320

Duan, H., Ma, R., Xu, X., Kong, F., Zhang, S., Kong, W., … Shang, L. (2009). Two-Decade Reconstruction of Algal Blooms in China's Lake Taihu. *Environmental Science & Technology*, *43*(10), 3522–3528. https://doi.org/10.1021/es8031852

Eppley. (1969). Half Saturation Constants for Uptake of Nitrate and Ammonia by Marine Phytoplankton. *Limnology and Oceanography.*

Filipe, C. D. M., & Daigger, G. T. (1999). Evaluation of the Capacity of Phosphorus-Accumulating Organisms to Use Nitrate and Oxygen as Final Electron Acceptors: A Theoretical Study on Population Dynamics. *Water Environment Research*, *71*(6), 1140–1150.

Fleck-Schneider, P., Lehr, F., & Posten, C. (2007). Modelling of growth and product formation of Porphyridium purpureum. *Journal of Biotechnology*, *132*(2), 134–141. https://doi.org/10.1016/j.jbiotec.2007.05.030

Gardner-Dale, D. A., Bradley, I. M., & Guest, J. S. (2017). Influence of solids residence time and carbon storage on nitrogen and phosphorus recovery by microalgae across diel cycles. *Water Research*, *121*, 231–239. https://doi.org/10.1016/j.watres.2017.05.033

Geider, R. J., & Osborne, B. A. (1989). Respiration and microalgal growth: a review of the quantitative relationship between dark respiration and growth. *New Phytologist*, *112*(3), 327–341. https://doi.org/10.1111/j.1469-8137.1989.tb00321.x

Gomes de Oliveira Dal'Molin, C., Quek, L.-E., Palfreyman, R. W., & Nielsen, L. K. (2011). AlgaGEM – a genome-scale metabolic reconstruction of algae based on the Chlamydomonas reinhardtii genome. *BMC Genomics*, *12*(4), S5. https://doi.org/10.1186/1471-2164-12-S4-S5

Gommers, P. J. F., van Schie, B. J., van Dijken, J. P., & Kuenen, J. G. (1988). Biochemical limits to microbial growth yields: An analysis of mixed substrate utilization. *Biotechnology and Bioengineering*, *32*(1), 86–94. https://doi.org/10.1002/bit.260320112

Guarnieri, M. t. (1), Darzins, A. (1, 5), Pienkos, P. t. (1), Nag, A. (2), Smolinski, S. l. (3), & Seibert, M. (4). (2011). Examination of triacylglycerol biosynthetic pathways via de novo transcriptomic and proteomic analyses in an unsequenced microalga. *PLoS ONE*, *6*(10). https://doi.org/10.1371/journal.pone.0025851

Guest, J. S., van Loosdrecht, M. C. M., Skerlos, S. J., & Love, N. G. (2013). Lumped Pathway Metabolic Model of Organic Carbon Accumulation and Mobilization by the Alga Chlamydomonas reinhardtii. *Environmental Science & Technology*, *47*(7), 3258–3267. https://doi.org/10.1021/es304980y

Hallegraeff, G. M. (1993). A review of harmful algal blooms and their apparent global increase. *Phycologia*, *32*(2), 79–99. https://doi.org/10.2216/i0031-8884-32-2-79.1

Henze, M. (1986). Activated Sludge Model No. 1. *Scientific and Technical Report No. 1, IAWQ*. Retrieved from https://ci.nii.ac.jp/naid/10003876234/

Henze, M., Gujer, W., Mino, T., & van Loosdrecht, M. C. M. (2000). *Activated sludge models ASM1, ASM2, ASM2d and ASM3*. London: IWA Publishing.

Hu, Q., Sommerfeld, M., Jarvis, E., Ghirardi, M., Posewitz, M., Seibert, M., & Darzins, A. (2008). Microalgal triacylglycerols as feedstocks for biofuel production: perspectives and advances. *The Plant Journal*, *54*(4), 621–639. https://doi.org/10.1111/j.1365-313X.2008.03492.x

Imam, S., Schäuble, S., Valenzuela, J., de Lomana, A. L. G., Carter, W., Price, N. D., & Baliga, N. S. (2015). A refined genome-scale reconstruction of Chlamydomonas metabolism provides a platform for systems-level analyses. *Plant Journal*, *84*(6), 1239–1256. https://doi.org/10.1111/tpj.13059

Imam, S., Schäuble, S., Valenzuela, J., López García de Lomana, A., Carter, W., Price, N. D., & Baliga, N. S. (2015). A refined genome-scale reconstruction of Chlamydomonas metabolism provides a platform for systems-level analyses. *The Plant Journal*, *84*(6), 1239–1256. https://doi.org/10.1111/tpj.13059

Jia, J., Han, D., Gerken, H. G., Li, Y., Sommerfeld, M., Hu, Q., & Xu, J. (2015). Molecular mechanisms for photosynthetic carbon partitioning into storage neutral lipids in Nannochloropsis oceanica

under nitrogen-depletion conditions. *Algal Research*, *7*, 66–77.

    https://doi.org/10.1016/j.algal.2014.11.005

Juneja, A., Chaplen, F. W. R., & Murthy, G. S. (2016). Genome scale metabolic reconstruction of Chlorella

    variabilis for exploring its metabolic potential for biofuels. *Bioresource Technology*, *213*, 103–

    110. https://doi.org/10.1016/j.biortech.2016.02.118

Juneja, A., & Murthy, G. S. (2018). Model predictive control coupled with economic and environmental

    constraints for optimum algal production. *Bioresource Technology*, *250*, 556–563.

    https://doi.org/10.1016/j.biortech.2017.11.047

Kamiya, A., & Kowallik, W. (1987). Photoinhibition of Glucose Uptake in Chlorella. *Plant and Cell*

    Physiology, *28*(4), 611–619. https://doi.org/10.1093/oxfordjournals.pcp.a077336

Kilian, O., Benemann, C. S. E., Niyogi, K. K., & Vick, B. (2011). High-efficiency homologous recombination

    in the oil-producing alga Nannochloropsis sp. *Proceedings of the National Academy of Sciences*,

    108(52), 21265–21269. https://doi.org/10.1073/pnas.1105861108

Koskimaki, J. E., Blazier, A. S., Clarens, A. F., & Papin, J. A. (2013). Computational Models of Algae

    Metabolism for Industrial Applications. *Industrial Biotechnology*, *9*(4), 185–195.

    https://doi.org/10.1089/ind.2013.0012

Krumholz, E. W., Yang, H., Weisenhorn, P., Henry, C. S., & Libourel, I. G. L. (2012). Genome-wide

    metabolic network reconstruction of the picoalga Ostreococcus. *Journal of Experimental Botany*,

    63(6), 2353–2362. https://doi.org/10.1093/jxb/err407

Lee, E., Jalalizadeh, M., & Zhang, Q. (2015). Growth kinetic models for microalgae cultivation: A review.

    Algal Research, *12*, 497–512. https://doi.org/10.1016/j.algal.2015.10.004

Leow, S., R. Witter, J., R. Vardon, D., K. Sharma, B., S. Guest, J., & J. Strathmann, T. (2015). Prediction of

    microalgae hydrothermal liquefaction products from feedstock biochemical composition. *Green*

    Chemistry, *17*(6), 3584–3599. https://doi.org/10.1039/C5GC00574D

Lewin, R. A. (c1962.). *Physiology and biochemistry of algae /*. New York : Academic Press,.

Li, Yalin, Leow, S., C. Fedders, A., K. Sharma, B., S. Guest, J., & J. Strathmann, T. (2017). Quantitative

    multiphase model for hydrothermal liquefaction of algal biomass. *Green Chemistry*, *19*(4), 1163–

    1174. https://doi.org/10.1039/C6GC03294J

Li, Yanqun, Horsman, M., Wang, B., Wu, N., & Lan, C. Q. (2008). Effects of nitrogen sources on cell

    growth and lipid accumulation of green alga Neochloris oleoabundans. *Applied Microbiology*

    and Biotechnology, *81*(4), 629–636. https://doi.org/10.1007/s00253-008-1681-1

Liang, Y., Sarkany, N., & Cui, Y. (2009). Biomass and lipid productivities of Chlorella vulgaris under autotrophic, heterotrophic and mixotrophic growth conditions. *Biotechnology Letters*, *31*(7), 1043–1049. https://doi.org/10.1007/s10529-009-9975-7

Manichaikul, A., Ghamsari, L., Hom, E. F. Y., Lin, C., Murray, R. R., Chang, R. L., … Papin, J. A. (2009). Metabolic network analysis integrated with transcript verification for sequenced genomes. *Nature Methods*, *6*(8), 589–592. https://doi.org/10.1038/nmeth.1348

Markou, G., Angelidaki, I., & Georgakakis, D. (2012). Microalgal carbohydrates: an overview of the factors influencing carbohydrates production, and of main bioconversion technologies for production of biofuels. *Applied Microbiology & Biotechnology*, *96*(3), 631–645. https://doi.org/10.1007/s00253-012-4398-0

Mata, T. M., Martins, A. A., & Caetano, N. S. (2010). Microalgae for biodiesel production and other applications: A review. *Renewable and Sustainable Energy Reviews*, *14*(1), 217–232. https://doi.org/10.1016/j.rser.2009.07.020

Meuser, J. E., Boyd, E. S., Ananyev, G., Karns, D., Radakovits, R., Narayana Murthy, U. M., … Posewitz, M. C. (2011). Evolutionary significance of an algal gene encoding an [FeFe]-hydrogenase with F-domain homology and hydrogenase activity in Chlorella variabilis NC64A. *Planta*, *234*(4), 829–843. https://doi.org/10.1007/s00425-011-1431-y

Murphy, T. E., & Berberoglu, H. (2014). Flux balancing of light and nutrients in a biofilm photobioreactor for maximizing photosynthetic productivity. *Biotechnology Progress*, *30*(2), 348–359. https://doi.org/10.1002/btpr.1881

Nelson, D. L., Lehninger, A. L., & Cox, M. M. (2008). *Lehninger Principles of Biochemistry*. Macmillan.

Noctor, G., & Foyer, C. H. (2000). Homeostasis of adenylate status during photosynthesis in a fluctuating environment. *Journal of Experimental Botany*, *51*(suppl_1), 347–356. https://doi.org/10.1093/jexbot/51.suppl_1.347

Paerl, H. W., Xu, H., McCarthy, M. J., Zhu, G., Qin, B., Li, Y., & Gardner, W. S. (2011). Controlling harmful cyanobacterial blooms in a hyper-eutrophic lake (Lake Taihu, China): The need for a dual nutrient (N & P) management strategy. *Water Research*, *45*(5), 1973–1983. https://doi.org/10.1016/j.watres.2010.09.018

Park, S., & Li, Y. (2015). Integration of biological kinetics and computational fluid dynamics to model the growth of Nannochloropsis salina in an open channel raceway. *Biotechnology and Bioengineering*, *112*(5), 923–933. https://doi.org/10.1002/bit.25509

Perez-Garcia, O., Bashan, Y., & Esther Puente, M. (2011). Organic Carbon Supplementation of Sterilized
Municipal Wastewater Is Essential for Heterotrophic Growth and Removing Ammonium by the
Microalga Chlorella Vulgaris1. *Journal of Phycology*, *47*(1), 190–199.
https://doi.org/10.1111/j.1529-8817.2010.00934.x

Pittman, J. K., Dean, A. P., & Osundeko, O. (2011). The potential of sustainable algal biofuel production
using wastewater resources. *Bioresource Technology*, *102*(1), 17–25.
https://doi.org/10.1016/j.biortech.2010.06.035

Rabalais, N. N., Turner, R. E., & Wiseman, W. J. (2002). Gulf of Mexico Hypoxia, A.K.A. "The Dead Zone."
Annual Review of Ecology and Systematics, *33*(1), 235–263.
https://doi.org/10.1146/annurev.ecolsys.33.010802.150513

Radakovits, R., Jinkerson, R. E., Fuerstenberg, S. I., Tae, H., Settlage, R. E., Boore, J. L., & Posewitz, M. C.
(2012). Draft genome sequence and genetic transformation of the oleaginous alga
Nannochloropsis gaditana. *Nature Communications*, *3*, 686.
https://doi.org/10.1038/ncomms1688

Rinta-Kanto, J. M., Konopko, E. A., DeBruyn, J. M., Bourbonniere, R. A., Boyer, G. L., & Wilhelm, S. W.
(2009). Lake Erie Microcystis: Relationship between microcystin production, dynamics of
genotypes and environmental parameters in a large lake. *Harmful Algae*, *8*(5), 665–673.
https://doi.org/10.1016/j.hal.2008.12.004

Roels, J. A. (1980). Application of macroscopic principles to microbial metabolism. *Biotechnology and
Bioengineering*, *22*(12), 2457–2514. https://doi.org/10.1002/bit.260221202

Roels, J. A. (1983). *Energetics and kinetics in biotechnology /*. Amsterdam ; Elsevier Biomedical Press,.

Ruhl, H. A., & Rybicki, N. B. (2010). Long-term reductions in anthropogenic nutrients link to
improvements in Chesapeake Bay habitat. *Proceedings of the National Academy of Sciences*,
107(38), 16566–16570. https://doi.org/10.1073/pnas.1003590107

Shastri, A. A., & Morgan, J. A. (2005). Flux Balance Analysis of Photoautotrophic Metabolism.
Biotechnology Progress, *21*(6), 1617–1626. https://doi.org/10.1021/bp050246d

Shen, Y., Yuan, W., Pei, Z., & Mao, E. (2010). Heterotrophic Culture of Chlorella protothecoides in
Various Nitrogen Sources for Lipid Production. *Applied Biochemistry and Biotechnology*, *160*(6),
1674–1684. https://doi.org/10.1007/s12010-009-8659-z

Skjånes, K., Rebours, C., & Lindblad, P. (2013). Potential for green microalgae to produce hydrogen,
pharmaceuticals and other high value products in a combined process. *Critical Reviews in
Biotechnology*, *33*(2), 172–215. https://doi.org/10.3109/07388551.2012.681625

Smolders, G. J. F., van der Meij, J., van Loosdrecht, M. C. M., & Heijnen, J. J. (1994). Stoichiometric model of the aerobic metabolism of the biological phosphorus removal process. *Biotechnology and Bioengineering*, *44*(7), 837–848. https://doi.org/10.1002/bit.260440709

Solimeno, A., Samsó, R., Uggetti, E., Sialve, B., Steyer, J.-P., Gabarró, A., & García, J. (2015). New mechanistic model to simulate microalgae growth. *Algal Research*, *12*, 350–358. https://doi.org/10.1016/j.algal.2015.09.008

Stouthamer, A. H. (1973a). A theoretical study on the amount of ATP required for synthesis of microbial cell material. *Antonie van Leeuwenhoek*, *39*(1), 545–565. https://doi.org/10.1007/BF02578899

Stouthamer, A. H. (1973b). A theoretical study on the amount of ATP required for synthesis of microbial cell material. *Antonie van Leeuwenhoek*, *39*(1), 545–565. https://doi.org/10.1007/BF02578899

Tchobanoglous, G., Burton, F. L., Stensel, H. D., & Metcalf & Eddy (Eds.). (2003). *Wastewater engineering: treatment and reuse* (4th ed). Boston: McGraw-Hill.

Tirichine, L., & Bowler, C. (2011). Decoding algal genomes: tracing back the history of photosynthetic life on Earth. *The Plant Journal*, *66*(1), 45–57. https://doi.org/10.1111/j.1365-313X.2011.04540.x

van Aalst-van Leeuwen, M. A., Pot, M. A., van Loosdrecht, M. C. M., & Heijnen, J. J. (1997a). Kinetic modeling of poly(β-hydroxybutyrate) production and consumption by Paracoccus pantotrophus under dynamic substrate supply. *Biotechnology and Bioengineering*, *55*(5), 773–782. https://doi.org/10.1002/(SICI)1097-0290(19970905)55:5<773::AID-BIT7>3.0.CO;2-8

van Aalst-van Leeuwen, M. A., Pot, M. A., van Loosdrecht, M. C. M., & Heijnen, J. J. (1997b). Kinetic modeling of poly(β-hydroxybutyrate) production and consumption by Paracoccus pantotrophus under dynamic substrate supply. *Biotechnology and Bioengineering*, *55*(5), 773–782. https://doi.org/10.1002/(SICI)1097-0290(19970905)55:5<773::AID-BIT7>3.0.CO;2-8

Verduyn, C., Stouthamer, A. H., Scheffers, W. A., & Dijken, J. P. van. (1991). A theoretical evaluation of growth yields of yeasts. *Antonie van Leeuwenhoek*, *59*(1), 49–63. https://doi.org/10.1007/BF00582119

Vieler, A., Guangxi Wu, Chia-Hong Tsai, Bullard, B., Cornish, A. J., Harvey, C., … Xiaobo Li. (2012). Genome, Functional Gene Annotation, and Nuclear Transformation of the Heterokont Oleaginous Alga Nannochloropsis oceanica CCMP1779. *PLoS Genetics*, *8*(11), 1–25. https://doi.org/10.1371/journal.pgen.1003064

Wágner, D. S., Valverde-Pérez, B., Sæbø, M., Bregua de la Sotilla, M., Van Wagenen, J., Smets, B. F., & Plósz, B. G. (2016). Towards a consensus-based biokinetic model for green microalgae – The ASM-A. *Water Research*, *103*, 485–499. https://doi.org/10.1016/j.watres.2016.07.026

Ward, A. J., Lewis, D. M., & Green, F. B. (2014). Anaerobic digestion of algae biomass: A review. *Algal Research*, *5*, 204–214. https://doi.org/10.1016/j.algal.2014.02.001

Wu, C., Xiong, W., Dai, J., & Wu, Q. (2015). Genome-Based Metabolic Mapping and 13C Flux Analysis Reveal Systematic Properties of an Oleaginous Microalga Chlorella protothecoides. *Plant Physiology*, *167*(2), 586–599. https://doi.org/10.1104/pp.114.250688

Xiong, W., Liu, L., Wu, C., Yang, C., & Wu, Q. (2010). 13C-Tracer and Gas Chromatography-Mass Spectrometry Analyses Reveal Metabolic Flux Distribution in the Oleaginous Microalga Chlorella protothecoides. *Plant Physiology*, *154*(2), 1001–1011. https://doi.org/10.1104/pp.110.158956

Yang, C., Hua, Q., & Shimizu, K. (2000). Energetics and carbon metabolism during growth of microalgal cells under photoautotrophic, mixotrophic and cyclic light-autotrophic/dark-heterotrophic conditions. *Biochemical Engineering Journal*, *6*(2), 87–102. https://doi.org/10.1016/S1369-703X(00)00080-2

Yang, J., Rasa, E., Tantayotai, P., Scow, K. M., Yuan, H., & Hristova, K. R. (2011). Mathematical model of Chlorella minutissima UTEX2341 growth and lipid production under photoheterotrophic fermentation conditions. *Bioresource Technology*, *102*(3), 3077–3082. https://doi.org/10.1016/j.biortech.2010.10.049

Zuñiga, C., Levering, J., Antoniewicz, M. R., Guarnieri, M. T., Betenbaugh, M. J., & Zengler, K. (2018). Predicting Dynamic Metabolic Demands in the Photosynthetic Eukaryote Chlorella vulgaris. *Plant Physiology*, *176*(1), 450–462. https://doi.org/10.1104/pp.17.00605

APPENDIX A. Supporting Material for "Development of Universal Stoichiometric Coefficients for Modeling Microalgal Cultivation Systems"

Table A.1 List of enzyme abbreviations used in enzyme conservation analysis

Enzyme	Abbreviation
Glycolysis	
Glucokinase (hexokinase)	GCK
Glucose -6 - Phosphate isomerase	GPI
6-phosphofructokinase	PFK
fructose biphosphate aldolase	FBA
Triose phosphate isomerase	TPI
glyceraldehyde-3-phosphate dehydrogenase	GAPDH
phosphoglycerate kinase	PGK
phosphoglycerate mutase	GPMA
phosphopyruvate hydratase (enolase)	ENO
pyruvate kinase	PK
Pentose Phosphate Pathway	
Glucose-6-Phosphate dehydrogenase	G6PD
6-phosphogluconolactonase	PGLS
phosphogluconate dehydrogenase	PGD
ribulose-phosphate 3-epimerase	RPE
ribose-5-phosphate isomerase	RPIA
transketolase	TKT
transaldolase	TALDO
Citric Acid/TCA Cycle	
pyruvate dehydrogenase	PDH
citrate synthase	CS
aconitate hydratase (aconitase)	ACON
isocitrate dehydrogenase	IDH
alpha-ketoglutarate dehydrogenase (2-oxoglutarate dehydrogenase)	OGDH
succinate-CoA ligase (succinyl CoA synthatase)	SUCLG
fumarate reductase	SDH
fumarate hydratase (fumerase)	FH
malate dehydrogenase	MDH
Photosynthesis Light Reactions	
photosystem 2	PS2
plastoquinol-plastocyanin reductase	Cb6f
photosystem 1	PS1
ferrodoxin NADP+ reductase	FNR
H+ transporting two sector ATPase	ATPase

Table A.1 (cont.)	
Calvin Cycle	
phosphoribulokinase	PRK
Ribulose-biphosphate carboxylase (RuBisCo)	RuBisCO
phosphoglycerate kinase	PGK
glyceraldehyde-3-phosphate dehydrogenase	GAPDH
Photorespiration	
Ribulose-biphosphate carboxylase (RuBisCo)	RuBisCO
phosphoglycolate phosphatase	PGP
2-hydroxy-acid oxidase (glycolate oxidase)	GLO
glycine transaminase (glyoxalate-glutamate aminotransferase)	GGT
glycine decarboxylase (aminomethyltransferase)	AMT
serine hydroxymethyltransferase	SHMT
serine aminotransferase	SGAT
glycerate dehydrogenase (hydroxypyruvate reductase/glycerate reductase)	GYDH
glycerate kinase	GLXK
glutamine synthetase and glutamate synthase	GLUL
Ammonia Assimilation	
glutamate-ammonia ligase (glutamine synthetase)	GLUL
glutamate synthase (NADH)	GLSN
Nitrate Assimilation	
nitrate reductase	NRA
ferrodoxin-nitrite reductase	NIR
Glyoxylate Cycle	
citrate (Si)-synthase	CS
aconitate hydratase (aconitase)	ACON
isocitrate lyase	ICL
malate synthase	MSN
malate dehydrogenase	MDH
Beta Oxidation	
acyl-CoA dehydrogenase	ACDH
enoyl-CoA hydratase	ECHD
beta-hydroxyacyl-CoA dehydrogenase	HADH
acyl-CoA C-acetyltransferase (thiolase)	ACAT
Fatty Acid Synthesis	
acetyl CoA carboxylase	ACAC
[acyl carrier protein] S-malonyltransferase	MCAT
beta-keoacyl-[acyl-carrier protein] synthase 1	FABB
[acyl carrier protein] reductase	FABG
Starch Synthesis	
glucose-1-phosphate adenylyltransferase	GLGC

Table A.1 (cont.)	
starch synthase	GLGA
1,4-alpha-glucan branching enzyme	GBE
Triacylglycerol Synthesis	
glycerol-3-phosphate 1-O-acyltransferase	GPAT
1-acylglycerol-3-phosphate O-acyltransferase	AGPAT
phosphatidate phosphatase	LPIN
diacylglycerol O-acyltransferase	DGAT
Gluconeogenesis	
pyruvate carboxylase	PC
malate dehydrogenase	MDH
malate dehydrogenase	MDH
phosphoenolpyruvate carboxykinase	PCK
phosphopyruvate hydratase	ENO
phosphoglycerate mutase	GPMA
phosphoglycerate kinase	PGK
glyceraldehyde-3-phosphate dehydrogenase	GAPDH
Triose phosphate isomerase	TPI
fructose biphosphate aldolase	FBA
fructose 1,6-biphosphatase	FBP
Glucose -6 - Phosphate isomerase	GPI
glucose-6-phosphatase	G6PC
Starch Degradation	
starch phosphorylase	PYGL
phosphoglucomutase	PGM
Triacylglycerol Degradation	
triacylglycerol lipase	GEH

Table A.2 Constant stoichiometric parameters used in lumped pathway metabolic model

Parameter	Description	Value	Units	Citations
δ_x	Carbon lost as atmospheric CO_2 for every c-mole of acetyl-CoA converted into biomass precursor	0.266	c-moles of CO_2 produced per c-mole of functional biomass	(Gommers, 1988; Smolders, 1994)
δ_n^{NH}	CO_2 production from the catabolism of acetyl-CoA to produce the required reducing power for converting nitrate to assimilable nitrogen	0.0	c-moles of CO_2 produced per c-mole of functional biomass	(Buchanan, 2015; Guest et al., 2013)
δ_n^{NO}	CO_2 production from the catabolism of acetyl-CoA to produce the required reducing power for converting nitrate to assimilable nitrogen	0.436	c-moles of CO_2 produced per c-mole of functional biomass	(Buchanan et al., 2015; Gomes de Oliveira Dal'Molin et al., 2011)
α_m	ATP utilization to convert acetyl-CoA to biomass precursor	0.65	moles ATP per c-mole of biomass precursor	(Stouthamer, 1973b)
α_x	ATP utilization to convert biomass precursor to functional biomass	1.5	moles ATP per c-mole of functional biomass	(van Aalst-van Leeuwen et al., 1997a; Verduyn et al., 1991)
δ_{PO}	P/O ratio; amount of ATP produced from NADH through the electron transport chain and oxidative phosphorylation	2.0	moles ATP produced per mole NADH oxidized	(Noctor & Foyer, 2000)
ϵ	ATP utilization to transport assimilable phosphorus in the form of orthophosphate into functional biomass	$0.11 \cdot \delta po$	moles ATP per mole of phosphate assimilated into c-mole of functional biomass	(Smolders et al., 1994)

Table A.3 List of metabolites involved in linear equations and the abbreviations used

Metabolite	Abbreviation	Units
Nicotinamide adenine dinucleotide (NADH)	r_{NADH}	$moles - (NADH) - hour^{-1}$
Adenosine triphosphate (ATP).	r_{ATP}	$moles - (ATP) - hour^{-1}$
Glucose-6-phosphate	r_{G6P}	$moles - (G6P \text{ as } C) - hour^{-1}$
Glyceraldehyde-3-phosphate	r_{G3P}	$moles - (G3P \text{ as } C) - hour^{-1}$
Acetyl-CoA	r_{ACoA}	$moles - (ACoA \text{ as } C) - hour^{-1}$
Biomass precursor	$r_{X_{pre}}$	$moles - (X_{pre} \text{ as } C) - hour^{-1}$
Functional biomass	$r_{X_{alg}}$	$moles - (X_{alg} \text{ as } C) - hour^{-1}$
Triacylglycerol (Lipid)	r_{TAG}	$moles - (TAG \text{ as } C) - hour^{-1}$
Polyglucose (carbohydrate)	r_{PG}	$moles - (PG \text{ as } C) - hour^{-1}$
Oxygen	r_{O_2}	$moles - (O_2) - hour^{-1}$
Carbon dioxide	r_{CO_2}	$moles - (CO_2 \text{ as } C) - hour^{-1}$

Table A.4 Linear equations for photoautotrophic nutrient-replete metabolism

#	Equation	Units
1[a]	$r_{NADH} = 0 = \frac{35}{51}r_{13} + \frac{11}{6}r_{14} - r_{15} + \frac{2}{3}r_2 + r_3(-0.1 + 2\delta_x)$	$moles - (NADH) - hour^{-1}$
2	$r_{ATP} = 0 = -\frac{1}{17}r_{13} + \frac{1}{2}r_{14} + \delta_{PO}r_{15} + \frac{2}{3}r_2 - \frac{1}{6}r_6$ $- \left(\alpha_x + \frac{m_{ATP}}{\mu_{max}}\right)r_4 + (-\alpha_M - (0.1\epsilon) + \frac{1}{2}\delta_n)r_3$	$moles - (ATP) - hour^{-1}$
3	$r_{G6P} = 0 = r_{10} - r_6$	$moles - (G6P\ as\ C) - hour^{-1}$
4	$r_{G3P} = 0 = r_1 - r_2 + r_6$	$moles - (G3P\ as\ C) - hour^{-1}$
5	$r_{ACoA} = 0 = r_{13} - r_{14} + \frac{2}{3}r_2 - r_3(1 + \delta_n + \delta_x)$	$moles - (ACoA\ as\ C) - hour^{-1}$
6	$r_{X_{pre}} = 0 = r_3 - r_4$	$moles - (X_{pre}\ as\ C) - hour^{-1}$
7	$r_{X_{alg}} = r_4$	$moles - (X_{alg}\ as\ C) - hour^{-1}$
8	$r_{TAG} = -r_{13}$	$moles - (TAG\ as\ C) - hour^{-1}$
9	$r_{PG} = -r_{10}$	$moles - (PG\ as\ C) - hour^{-1}$
10	$r_{O_2} = r_1 - \frac{1}{2}r_{15}$	$moles - (O_2) - hour^{-1}$
11	$r_{CO_2} = -r_1 + r_{14} + \frac{1}{3}r_2 + (\delta_n + \delta_x)r_3$	$moles - (CO_2\ as\ C) - hour^{-1}$
12[b]	$4r_{O_2} = \frac{290}{51}r_{TAG} + 4r_{PG} + 4.2r_{X_{alg}}$	-

[a] Assumes $FADH_2 = \frac{2}{3}NADH$ and $NADH_2 = NADH$

[b] Degree of Reduction balance based on Roels, 1983 and Nielsen, 1995. . In #12, the coefficient for $r_{X_{alg}}$ is 5.8 when nitrate is the nitrogen source.

Table A.5 Linear equations for photoautotrophic nutrient-deplete metabolism

#	Equation	Units
1[a]	$r_{NADH} = 0 = -\frac{14}{17}r_{12} + \frac{11}{6}r_{14} - r_{15} + r_7 + \frac{2}{3}r_2 + (-0.1 + 2\delta_x)r_3$	$moles - (NADH) - hour^{-1}$
2	$r_{ATP} = 0 = -\frac{1}{6}r_9 - \frac{8}{17}r_{12} + \frac{1}{2}r_{14} + \delta_{PO}r_{15} + \frac{2}{3}r_2 - \left(\alpha_x + \frac{m_{ATP}}{\mu_{max}}\right)r_4 + (-\alpha_M - (0.1\epsilon) + \frac{1}{2}\delta_n)r_3$	$moles - (ATP) - hour^{-1}$
3	$r_{G6P} = 0 = r_7 + r_9$	$moles - (G6P\ as\ C) - hour^{-1}$
4	$r_{G3P} = 0 = r_1 - r_2 + \frac{1}{2}r_7$	$moles - (G3P\ as\ C) - hour^{-1}$
5	$r_{ACoA} = 0 = -r_{12} - r_{14} + \frac{2}{3}r_2 - r_3(1 + \delta_n + \delta_x)$	$moles - (ACoA\ as\ C) - hour^{-1}$
6	$r_{X_{pre}} = 0 = r_3 - r_4$	$moles - (X_{pre}\ as\ C) - hour^{-1}$
7	$r_{X_{alg}} = r_4$	$moles - (X_{alg}\ as\ C) - hour^{-1}$
8	$r_{TAG} = r_{12}$	$moles - (TAG\ as\ C) - hour^{-1}$
9	$r_{PG} = r_9$	$moles - (PG\ as\ C) - hour^{-1}$
10	$r_{CO_2} = -r_1 + r_{14} + \frac{1}{3}r_2 + \frac{1}{2}r_7 + (\delta_n + \delta_x)r_3$	$moles - (O_2) - hour^{-1}$
11	$r_{O_2} = r_1 - \frac{1}{2}r_{15}$	$moles - (CO_2) - hour^{-1}$
12[b]	$4r_{o_2} = \frac{290}{51}r_{TAG} + 4r_{PG} + 4.2r_{X_{alg}}$	-

[a] Assumes $FADH_2 = \frac{2}{3}NADH$ and $NADH_2 = NADH$

[b] Degree of Reduction balance based on Roels, 1983 and Nielsen, 1995. . In #12, the coefficient for r_{Xalg} is 5.8 when nitrate is the nitrogen source.

Table A.6 Linear equations for heterotrophic with acetate nutrient-replete metabolism

#	Equation	Units
1[a]	$r_{NADH} = 0 = \frac{35}{51}r_{13} + \frac{11}{6}r_{14} - r_{15} + \frac{2}{3}r_2 + r_7 + (-0.1 + 2\delta_x)r_3$	$moles - (NADH) - hour^{-1}$
2	$r_{ATP} = 0 = -\frac{1}{2}r_{11} - \frac{1}{17}r_{13} + \frac{1}{2}r_{14} + \delta_{PO}r_{15} + \frac{2}{3}r_2 - \left(\alpha_x + \frac{m_{ATP}}{\mu_{max}}\right)r_4 + (-\alpha_M - (0.1\epsilon) + \frac{1}{2}\delta_n)r_3$	$moles - (ATP) - hour^{-1}$
3	$r_{G6P} = 0 = r_{10} + r_8 - r_7$	$moles - (G6P\ as\ C) - hour^{-1}$
4	$r_{G3P} = 0 = -r_2 + \frac{1}{2}r_7 - r_8$	$moles - (G3P\ as\ C) - hour^{-1}$
5	$r_{ACoA} = 0 = r_{11} - r_{14} + \frac{2}{3}r_2 - r_3(1 + \delta_n + \delta_x) + r_{13}$	$moles - (ACoA\ as\ C) - hour^{-1}$
6	$r_{X_{pre}} = 0 = r_3 - r_4$	$moles - (X_{pre}\ as\ C) - hour^{-1}$
7	$r_{X_{alg}} = r_4$	$moles - (X_{alg}\ as\ C) - hour^{-1}$
8	$r_{TAG} = -r_{13}$	$moles - (TAG\ as\ C) - hour^{-1}$
9	$r_{PG} = -r_{10}$	$moles - (PG\ as\ C) - hour^{-1}$
10	$r_{O_2} = -\frac{1}{2}r_{15}$	$moles - (O_2) - hour^{-1}$
11	$r_{CO_2} = r_{14} + \frac{1}{3}r_2 + \frac{1}{2}r_7 + (\delta_n + \delta_x)r_3$	$moles - (CO_2) - hour^{-1}$
12	$r_{AC} = -r_{11}$	$moles - (AC) - hour^{-1}$
13[b]	$4r_{O_2} = 4r_{ac} + \frac{290}{51}r_{TAG} + 4r_{PG} + 4.2r_{X_{alg}}$	-

[a] Assumes $FADH_2 = \frac{2}{3}NADH$ and $NADH_2 = NADH$

[b] Degree of Reduction balance based on Roels, 1983 and Nielsen, 1995. . In #12, the coefficient for r_{Xalg} is 5.8 when nitrate is the nitrogen source.

Table A.7 Linear equations for heterotrophic with acetate nutrient-deplete metabolism

#	Equation	Units
1[a]	$r_{NADH} = 0 = -\frac{14}{17}r_{12} + \frac{11}{6}r_{14} - r_{15} + \frac{2}{3}r_2 + r_7 + (-0.1 + 2\delta_x)r_3$	$moles - (NADH) - hour^{-1}$
2	$r_{ATP} = 0 = -\frac{1}{6}r_9 - \frac{1}{2}r_{11} - \frac{8}{17}r_{12} + \frac{1}{2}r_{14} + \delta_{PO}r_{15} + \frac{2}{3}r_2 - \left(\alpha_x + \frac{m_{ATP}}{\mu_{max}}\right)r_4 + \left(-\alpha_M - (0.1\epsilon) + \frac{1}{2}\delta_n\right)r_3$	$moles - (ATP) - hour^{-1}$
3	$r_{G6P} = 0 = r_8 - r_7 - r_9$	$moles - (G6P\ as\ C) - hour^{-1}$
4	$r_{G3P} = 0 = -r_2 + \frac{1}{2}r_7 - r_8$	$moles - (G3P\ as\ C) - hour^{-1}$
5	$r_{ACoA} = 0 = r_{11} - r_{12} - r_{14} + \frac{2}{3}r_2 - r_3(1 + \delta_n + \delta_x)$	$moles - (ACoA\ as\ C) - hour^{-1}$
6	$r_{X_{pre}} = 0 = r_3 - r_4$	$moles - (X_{pre}\ as\ C) - hour^{-1}$
7	$r_{X_{alg}} = r_4$	$moles - (X_{alg}\ as\ C) - hour^{-1}$
8	$r_{TAG} = r_{12}$	$moles - (TAG\ as\ C) - hour^{-1}$
9	$r_{PG} = r_9$	$moles - (PG\ as\ C) - hour^{-1}$
10	$r_{O_2} = -\frac{1}{2}r_{15}$	$moles - (O_2) - hour^{-1}$
11	$r_{CO_2} = r_{14} + \frac{1}{3}r_2 + \frac{1}{2}r_7 + (\delta_n + \delta_x)r_3$	$moles - (CO_2) - hour^{-1}$
12	$r_{AC} = -r_{11}$	$moles - (AC) - hour^{-1}$
13[b]	$4r_{O_2} = 4r_{ac} + \frac{290}{51}r_{TAG} + 4r_{PG} + 4.2r_{X_{alg}}$	-

[a] Assumes $FADH_2 = \frac{2}{3}NADH$ and $NADH_2 = NADH$

[b] Degree of Reduction balance based on Roels, 1983 and Nielsen, 1995. . In #12, the coefficient for r_{Xalg} is 5.8 when nitrate is the nitrogen source.

Table A.8 Linear equations for heterotrophic with glucose nutrient-replete metabolism

#	Equation	Units
1[a]	$r_{NADH} = 0 = \frac{35}{51}r_{13} + \frac{11}{6}r_{14} - r_{15} + \frac{2}{3}r_2 + r_7 + (-0.1 + 2\delta_x)r_3$	$moles - (NADH) - hour^{-1}$
2	$r_{ATP} = 0 = -\frac{1}{17}r_{13} + \frac{1}{2}r_{14} + \delta_{PO}r_{15} + \frac{2}{3}r_2 - \left(\alpha_x + \frac{m_{ATP}}{\mu_{max}}\right)r_4 - \frac{1}{3}r_5 + (-\alpha_M - (0.1\epsilon) + \frac{1}{2}\delta_n)r_3$	$moles - (ATP) - hour^{-1}$
3	$r_{G6P} = 0 = r_{10} + r_5 + r_8 - r_7$	$moles - (G6P \text{ as } C) - hour^{-1}$
4	$r_{G3P} = 0 = -r_2 + \frac{1}{2}r_7 - r_8$	$moles - (G3P \text{ as } C) - hour^{-1}$
5	$r_{ACoA} = 0 = r_{13} - r_{14} + \frac{2}{3}r_2 - r_3(1 + \delta_n + \delta_x)$	$moles - (ACoA \text{ as } C) - hour^{-1}$
6	$r_{X_{pre}} = 0 = r_3 - r_4$	$moles - (X_{pre} \text{ as } C) - hour^{-1}$
7	$r_{X_{alg}} = r_4$	$moles - (X_{alg} \text{ as } C) - hour^{-1}$
8	$r_{TAG} = -r_{13}$	$moles - (TAG \text{ as } C) - hour^{-1}$
9	$r_{PG} = -r_{10}$	$moles - (PG \text{ as } C) - hour^{-1}$
10	$r_{O_2} = -\frac{1}{2}r_{15}$	$moles - (O_2) - hour^{-1}$
11	$r_{CO_2} = r_{14} + \frac{1}{3}r_2 + \frac{1}{2}r_7 + (\delta_n + \delta_x)r_3$	$moles - (CO_2) - hour^{-1}$
12	$r_{GLC} = -r_5$	$moles - (GLC) - hour^{-1}$
13[b]	$4r_{O_2} = 4r_{glc} + \frac{290}{51}r_{TAG} + 4r_{PG} + 4.2r_{X_{alg}}$	-

[a] Assumes $FADH_2 = \frac{2}{3}NADH$ and $NADH_2 = NADH$

[b] Degree of Reduction balance based on Roels, 1983 and Nielsen, 1995. . In #12, the coefficient for r_{Xalg} is 5.8 when nitrate is the nitrogen source.

Table A.9 Linear equations for heterotrophic with glucose nutrient-deplete metabolism

#	Equation	Units
1[a]	$r_{NADH} = 0 = -\frac{14}{17}r_{12} + \frac{11}{6}r_{14} - r_{15} + \frac{2}{3}r_2 + r_7 + (-0.1 + 2\delta_x)r_3$	$moles - (NADH) - hour^{-1}$
2	$r_{ATP} = 0 = -\frac{8}{17}r_{12} + \frac{1}{2}r_{14} + \delta_{PO}r_{15} + \frac{2}{3}r_2 - \frac{1}{3}r_5 - \frac{1}{6}r_9 - \left(\alpha_x + \frac{m_{ATP}}{\mu_{max}}\right)r_4 + (-\alpha_M - (0.1\epsilon) + \frac{1}{2}\delta_n)r_3$	$moles - (ATP) - hour^{-1}$
3	$r_{G6P} = 0 = r_5 + r_8 - r_7 - r_9$	$moles - (G6P\ as\ C) - hour^{-1}$
4	$r_{G3P} = 0 = -r_2 + \frac{1}{2}r_7 - r_8$	$moles - (G3P\ as\ C) - hour^{-1}$
5	$r_{ACoA} = 0 = -r_{12} - r_{14} + \frac{2}{3}r_2 - r_3(1 + \delta_n + \delta_x)$	$moles - (ACoA\ as\ C) - hour^{-1}$
6	$r_{X_{pre}} = 0 = r_3 - r_4$	$moles - (X_{pre}\ as\ C) - hour^{-1}$
7	$r_{X_{alg}} = r_4$	$moles - (X_{alg}\ as\ C) - hour^{-1}$
8	$r_{TAG} = r_{12}$	$moles - (TAG\ as\ C) - hour^{-1}$
9	$r_{PG} = r_9$	$moles - (PG\ as\ C) - hour^{-1}$
10	$r_{O_2} = -\frac{1}{2}r_{15}$	$moles - (O_2) - hour^{-1}$
11	$r_{CO_2} = r_{14} + \frac{1}{3}r_2 + \frac{1}{2}r_7 + (\delta_n + \delta_x)r_3$	$moles - (CO_2) - hour^{-1}$
12	$r_{GLC} = -r_5$	$moles - (GLC) - hour^{-1}$
13[b]	$4r_{O_2} = 4r_{glc} + \frac{290}{51}r_{TAG} + 4r_{PG} + 4.2r_{X_{alg}}$	-

[a] Assumes $FADH_2 = \frac{2}{3}NADH$ and $NADH_2 = NADH$

[b] Degree of Reduction balance based on Roels, 1983 and Nielsen, 1995. . In #12, the coefficient for r_{Xalg} is 5.8 when nitrate is the nitrogen source.

Table A.10 Linear equations for heterotrophic with stored biopolymers nutrient-replete metabolism

#	Equation	Units
1[a]	$r_{NADH} = 0 = \frac{35}{51}r_{13} + \frac{11}{6}r_{14} - r_{15} + \frac{2}{3}r_2 + r_7 + (-0.1 + 2\delta_x)r_3$	$moles - (NADH) - hour^{-1}$
2	$r_{ATP} = 0 = -\frac{1}{17}r_{13} + \frac{1}{2}r_{14} + \delta_{PO}r_{15} + \frac{2}{3}r_2 - \left(\alpha_x + \frac{m_{ATP}}{\mu_{max}}\right)r_4 + (-\alpha_M - (0.1\epsilon) + \frac{1}{2}\delta_n)r_3$	$moles - (ATP) - hour^{-1}$
3	$r_{G6P} = 0 = r_{10} + r_8 - r_7$	$moles - (G6P\ as\ C) - hour^{-1}$
4	$r_{G3P} = 0 = \frac{1}{2}r_7 - r_2 - r_8$	$moles - (G3P\ as\ C) - hour^{-1}$
5	$r_{ACoA} = 0 = -r_{14} + r_{13} + \frac{2}{3}r_2 - r_3(1 + \delta_n + \delta_x)$	$moles - (ACoA\ as\ C) - hour^{-1}$
6	$r_{X_{pre}} = 0 = r_3 - r_4$	$moles - (X_{pre}\ as\ C) - hour^{-1}$
7	$r_{X_{alg}} = r_4$	$moles - (X_{alg}\ as\ C) - hour^{-1}$
8	$r_{TAG} = -r_{13}$	$moles - (TAG\ as\ C) - hour^{-1}$
9	$r_{PG} = -r_{10}$	$moles - (PG\ as\ C) - hour^{-1}$
10	$r_{O_2} = -\frac{1}{2}r_{15}$	$moles - (O_2) - hour^{-1}$
11	$r_{CO_2} = r_{14} + \frac{1}{3}r_2 + \frac{1}{2}r_7 + (\delta_n + \delta_x)r_3$	$moles - (CO_2) - hour^{-1}$
12[b]	$4r_{O_2} = \frac{290}{51}r_{TAG} + 4r_{PG} + 4.2r_{X_{alg}}$	-

[a] Assumes $FADH_2 = \frac{2}{3}NADH$ and $NADH_2 = NADH$

[b] Degree of Reduction balance based on Roels, 1983 and Nielsen, 1995. . In #12, the coefficient for r_{Xalg} is 5.8 when nitrate is the nitrogen source.

Table A.11 Linear equation solutions for photoautotrophic metabolism

Description [units]	Nutrient-Replete Metabolism	Nutrient-Deplete Metabolism
Specific Rate of Photosynthesis [moles-(CO₂ fixed to G3P)·moles-(X_alg as C)⁻¹·hour⁻¹]	$q_{PHOT}^{NR} = \dfrac{\mu^{NR}}{Y_{X_{alg}}^{NR}} + \dfrac{q_{PG}^{NR}}{Y_{PG}^{NR}} + \dfrac{q_{TAG}^{NR}}{Y_{TAG}^{NR}} + \dfrac{m_{ATP}^{NR}}{Y_{ATP}^{NR}}$	$q_{PHOT}^{ND} = \dfrac{\mu^{ND}}{Y_{X_{alg}}^{ND}} + \dfrac{q_{PG}^{ND}}{Y_{PG}^{ND}} + \dfrac{q_{TAG}^{ND}}{Y_{TAG}^{ND}} + \dfrac{m_{ATP}^{ND}}{Y_{ATP}^{ND}}$
Specific Rate of CO₂ Production [moles-(CO₂)·moles-(X_alg as C)⁻¹·hour⁻¹]	$q_{CO_2}^{NR} = -q_{PG}^{NR} - q_{TAG}^{NR} - \mu^{NR}$	$q_{CO_2}^{ND} = -q_{PG}^{ND} - q_{TAG}^{ND} - \mu^{ND}$
Specific Rate of O₂ Production [moles-(O₂)·moles-(X_alg as C)⁻¹·hour⁻¹]	$q_{O_2}^{NH} = q_{PG}^{NH} + \frac{145}{102}q_{TAG}^{NH} + \frac{21}{20}\mu^{NH}$ $q_{O_2}^{NO} = q_{PG}^{NO} + \frac{145}{102}q_{TAG}^{NO} + \frac{29}{20}\mu^{NO}$	$q_{O_2}^{ND} = q_{PG}^{ND} + \frac{145}{102}q_{TAG}^{ND} + \frac{21}{20}\mu^{ND}$

Note on superscripts: NH; ammonia as nitrogen source, NO; nitrate as nitrogen source, NR; nitrogen source present, could be ammonia or nitrate, ND; no nitrogen source present

q_{phot}; specific rate of CO₂ fixation to G3P, moles-(G3P as C)·mole-(X_alg as C)⁻¹·hr⁻¹

q_{CO2}; specific rate of CO₂ production, moles-(CO₂)·mole-(X_alg as C)⁻¹·hr⁻¹

q_{O2}; specific rate of O₂ production, moles-(O₂)·mole-(X_alg as C)⁻¹·hr⁻¹

Additional note: Specific rate equations described using parameter q (specific rate of production), Y (yield coefficient), and μ (functional biomass growth rate). Constant parameters descriptions and values can be found in table A.2.

Table A.12 Linear equation solutions for heterotrophic metabolism with acetate

Description [units]	Nutrient-Replete Metabolism	Nutrient-Deplete Metabolism
Specific Rate of Acetate Fixation [moles-(Acetate fixed to Acetyl-CoA)·moles-(X_alg as C)⁻¹·hour⁻¹]	$q_{Ac}^{NR} = \dfrac{\mu^{NR}}{Y_{X_{alg}}^{NR}} + \dfrac{q_{PG}^{NR}}{Y_{PG}^{NR}} + \dfrac{q_{TAG}^{NR}}{Y_{TAG}^{NR}} + \dfrac{m_{ATP}^{NR}}{Y_{ATP}^{NR}}$	$q_{Ac}^{ND} = \dfrac{\mu^{ND}}{Y_{X_{alg}}^{ND}} + \dfrac{q_{PG}^{ND}}{Y_{PG}^{ND}} + \dfrac{q_{TAG}^{ND}}{Y_{TAG}^{ND}} + \dfrac{m_{ATP}^{ND}}{Y_{ATP}^{ND}}$
Specific Rate of CO₂ Production [moles-(CO₂)·moles-(X_alg as C)⁻¹·hour⁻¹]	$q_{CO_2}^{NR} = -q_{Ac}^{NR} - q_{PG}^{NR} - q_{TAG}^{NR} - \mu^{NR}$	$q_{CO_2}^{ND} = -q_{Ac}^{ND} - q_{PG}^{ND} - q_{TAG}^{ND} - \mu^{ND}$
Specific Rate of O₂ Production [moles-(O₂)·moles-(X_alg as C)⁻¹·hour⁻¹]	$q_{O_2}^{NH} = q_{Ac}^{NH} + q_{PG}^{NH} + \frac{145}{102}q_{TAG}^{NH} + \frac{21}{20}\mu^{NH}$ $q_{O_2}^{NO} = q_{Ac}^{NO} + q_{PG}^{NO} + \frac{145}{102}q_{TAG}^{NO} + \frac{29}{20}\mu^{NO}$	$q_{O_2}^{ND} = q_{Ac}^{ND} + q_{PG}^{ND} + \frac{145}{102}q_{TAG}^{ND} + \frac{21}{20}\mu^{ND}$

Note on superscripts: NH; ammonia as nitrogen source, NO; nitrate as nitrogen source, NR; nitrogen source present, could be ammonia or nitrate, ND; no nitrogen source present

q_{Ac}; specific rate of acetate fixation to acetyl-CoA, moles-(acetyl-CoA as C)·mole-(X_alg as C)⁻¹·hr⁻¹

q_{CO2}; specific rate of CO₂ production, moles-(CO₂)·mole-(X_alg as C)⁻¹·hr⁻¹

q_{O2}; specific rate of O₂ production, moles-(O₂)·mole-(X_alg as C)⁻¹·hr⁻¹

Additional note: Specific rate equations described using parameter q (specific rate of production), Y (yield coefficient), and μ (functional biomass growth rate). Constant parameters descriptions and values can be found in table A.2.

Table A.13 Linear equation solutions for heterotrophic metabolism with glucose

Description [units]	Nutrient-Replete Metabolism	Nutrient-Deplete Metabolism
Specific Rate of Glucose Fixation [moles-(Glucose fixed to G6P)·moles-(X_{alg} as C)$^{-1}$·hour^{-1}]	$q_{GLC}^{NR} = \dfrac{\mu^{NR}}{Y_{X_{alg}}^{NR}} + \dfrac{q_{PG}^{NR}}{Y_{PG}^{NR}} + \dfrac{q_{TAG}^{NR}}{Y_{TAG}^{NR}} + \dfrac{m_{ATP}^{NR}}{Y_{ATP}^{NR}}$	$q_{GLC}^{ND} = \dfrac{\mu^{ND}}{Y_{X_{alg}}^{ND}} + \dfrac{q_{PG}^{ND}}{Y_{PG}^{ND}} + \dfrac{q_{TAG}^{ND}}{Y_{TAG}^{ND}} + \dfrac{m_{ATP}^{ND}}{Y_{ATP}^{ND}}$
Specific Rate of CO_2 Production [moles-(CO_2)·moles-(X_{alg} as C)$^{-1}$·hour^{-1}]	$q_{CO_2}^{NR} = -q_{GLC}^{NR} - q_{PG}^{NR} - q_{TAG}^{NR} - \mu^{NR}$	$q_{CO_2}^{ND} = -q_{GLC}^{ND} - q_{PG}^{ND} - q_{TAG}^{ND} - \mu^{ND}$
Specific Rate of O_2 Production [moles-(O_2)·moles-(X_{alg} as C)$^{-1}$·hour^{-1}]	$q_{O_2}^{NH} = q_{GLC}^{NH} + q_{PG}^{NH} + \frac{145}{102}q_{TAG}^{NH} + \frac{21}{20}\mu^{NH}$ $q_{O_2}^{NO} = q_{GLC}^{NO} + q_{PG}^{NO} + \frac{145}{102}q_{TAG}^{NO} + \frac{21}{20}\mu^{NO}$	$q_{O_2}^{ND} = q_{GLC}^{ND} + q_{PG}^{ND} + \frac{145}{102}q_{TAG}^{ND} + \frac{21}{20}\mu^{ND}$

Note on superscripts: NH; ammonia as nitrogen source, NO; nitrate as nitrogen source, NR; nitrogen source present, could be ammonia or nitrate, ND; no nitrogen source present

q_{GLC}; specific rate of glucose fixation to G6P, moles-(G6P as C)·mole-(X_{alg} as C)$^{-1}$·hr^{-1}

q_{CO2}; specific rate of CO_2 production, moles-(CO_2)·mole-(X_{alg} as C)$^{-1}$·hr^{-1}

q_{O2}; specific rate of O_2 production, moles-(O_2)·mole-(X_{alg} as C)$^{-1}$·hr^{-1}

Additional note: Specific rate equations described using parameter q (specific rate of production), Y (yield coefficient), and μ (functional biomass growth rate). Constant parameters descriptions and values can be found in table A.2.

Table A.14 Stoichiometric yields derived from linear equation solutions for photoautotrophic metabolism

Description [units]	Nutrient-Replete Metabolism	Nutrient-Deplete Metabolism
yield of polyglucose on CO_2 fixed to G3P [(C-moles PG)·(C-mole CO_2 fixed to G3P)$^{-1}$]	$Y^{NR}_{PG} = \dfrac{18 + 34\delta_{PO}}{15 + 34\delta_{PO}}$	$Y^{ND}_{PG} = \dfrac{18 + 34\delta_{PO}}{12 + 35\delta_{PO}}$
yield of lipid on CO_2 fixed to G3P [(C-moles LI)·(C-mole CO_2 fixed to G3P)$^{-1}$]	$Y^{NR}_{LI} = \dfrac{306 + 578\delta_{PO}}{135 + 771\delta_{PO}}$	$Y^{ND}_{LI} = \dfrac{306 + 578\delta_{PO}}{297 + 813\delta_{PO}}$
yield of biomass on CO_2 fixed to G3P [(C-moles biomass)·(C-mole CO_2 fixed to G3P)$^{-1}$]^{a}	$Y_{X_{alg\_NH}}$ $= \dfrac{170\delta_{PO} + 90}{90\alpha_M + 90\alpha_x + 90(0.1\epsilon) + 174\delta_{PO} + 165\delta_n^{NH}\delta_{PO} + 45\delta_x - 15\delta_{PO}\delta_x + 45}$ $Y_{X_{alg\_NO}}$ $= \dfrac{170\delta_{PO} + 90}{90\alpha_M + 90\alpha_x + 90(0.1\epsilon) + 174\delta_{PO} + 165\delta_n^{NO}\delta_{PO} + 45\delta_x - 15\delta_{PO}\delta_x + 45}$	
yield of ATP on CO_2 fixed to G3P [(moles of ATP)·(C-mole CO_2 fixed to G3P)$^{-1}$]	$Y^{NR}_{ATP} = \dfrac{9 + 17\delta_{PO}}{9}$	$Y^{ND}_{ATP} = \dfrac{9 + 17\delta_{PO}}{9}$

[a] Yield of biomass can only happen under nutrient replete conditions

Note: Constant parameters descriptions and values can be found in table A.2

Table A.15 Stoichiometric yields derived from linear equation solutions for heterotrophic metabolism with acetate

Description [units]	Nutrient-Replete Metabolism	Nutrient-Deplete Metabolism
yield of polyglucose on acetate fixed to acetyl-CoA [(C-moles PG)·(C-mole acetate fixed to acetyl-CoA)$^{-1}$]	$Y_{\overline{PG}}^{NR} = \dfrac{4\delta_{PO} - 3}{4\delta_{PO}}$	$Y_{\overline{PG}}^{ND} = \dfrac{12\delta_{PO} - 9}{12\delta_{PO} + 1}$
yield of lipid on acetate fixed to acetyl-CoA [(C-moles LI)·(C-mole acetate fixed to acetyl-CoA)$^{-1}$]	$Y_{\overline{LI}}^{NR} = \dfrac{204\delta_{PO} - 153}{290\delta_{PO} - 252}$	$Y_{\overline{LI}}^{ND} = \dfrac{204\delta_{PO} - 153}{290\delta_{PO} - 72}$
yield of biomass on acetate fixed to acetyl-CoA [(C-moles biomass)·(C-mole acetate fixed to acetyl-CoA)$^{-1}$]^{a}	$Y_{X_{alg\_NH}} = \dfrac{2040\delta_{PO} - 1530}{1020(\alpha_m + \alpha_x + (0.1\epsilon) - \delta_x) + 16830\delta_n^{NH} + 2142\delta_{PO} - 1020}$ $Y_{X_{alg\_NO}} = \dfrac{2040\delta_{PO} - 1530}{1020(\alpha_m + \alpha_x + (0.1\epsilon) - \delta_x) + 16830\delta_n^{NO} + 2958\delta_{PO} - 8364}$	
yield of ATP on acetate fixed to acetyl-CoA [(moles of ATP)·(C-mole acetate fixed to acetyl-CoA)$^{-1}$]	$Y_{\overline{ATP}}^{NR} = \dfrac{4\delta_{PO} - 3}{2}$	$Y_{\overline{ATP}}^{ND} = \dfrac{4\delta_{PO} - 3}{2}$

^{a} Yield of biomass can only happen under nutrient replete conditions

Note: Constant parameters descriptions and values can be found in table A.2

Table A.16 Stoichiometric yields derived from linear equation solutions for heterotrophic metabolism with glucose

Description [units]	Nutrient-Replete Metabolism	Nutrient-Deplete Metabolism
yield of polyglucose on glucose fixed to G6P [(C-moles PG)·(C-mole glucose fixed to G6))$^{-1}$]	$Y_{PG}^{NR} = \dfrac{6 - \delta_{PO}}{6}$	$Y_{PG}^{ND} = \dfrac{12\delta_{PO} - 2}{12\delta_{PO} + 1}$
yield of lipid on glucose fixed to G6P [(C-moles LI)·(C-mole glucose fixed to G6P)$^{-1}$]	$Y_{LI}^{NR} = \dfrac{102\delta_{PO} - 17}{145\delta_{PO} - 126}$	$Y_{LI}^{ND} = \dfrac{102\delta_{PO} - 17}{145\delta_{PO} - 36}$
yield of biomass on glucose fixed to G6P [(C-moles biomass)·(C-mole glucose fixed to G6P)$^{-1}$]^a	$Y_{X_{alg\_NH}} = \dfrac{1020\delta_{PO} - 170}{510(\alpha_m + \alpha_x + (0.1\epsilon) - \delta_x) + 8415\delta_n^{NH} + 1071\delta_{PO} - 510}$ $Y_{X_{alg\_NO}} = \dfrac{1020\delta_{PO} - 170}{510(\alpha_m + \alpha_x + (0.1\epsilon) - \delta_x) + 8415\delta_n^{NO} + 1479\delta_{PO} - 4182}$	
yield of ATP on glucose fixed to G6P [(moles of ATP)·(C-mole glucose fixed to G6P)$^{-1}$]	$Y_{ATP}^{NR} = \dfrac{6\delta_{PO} - 1}{3}$	$Y_{ATP}^{ND} = \dfrac{6\delta_{PO} - 1}{3}$

^{a} Yield of biomass can only happen under nutrient replete conditions

Note: Constant parameters descriptions and values can be found in table A.2